ANKARA YILDIRIM BEYAZIT UNIVERSITY

GRADUATE SCHOOL OF NATURAL AND APPLIED SCIENCES

EFFECT OF TEMPERING CONDITIONS ON THE FINAL PROPERTIES OF BALL BEARINGS

M.Sc. Thesis by

Buğra İPEK

Department of Materials Engineering

November, 2021

ANKARA

EFFECT OF TEMPERING CONDITIONS ON THE FINAL PROPERTIES OF BALL BEARINGS

A Thesis Submitted to

The Graduate School of Natural and Applied Sciences of

Ankara Yıldırım Beyazıt University

In Partial Fulfillment of the Requirements for the Degree of Master of Science in Material Engineering, Department of Material Engineering

by

Buğra İPEK

November, 2021

ANKARA

M. Sc. THESIS EXAMINATION RESULT FORM

We have read the thesis entitled "**EFFECT OF TEMPERING CONDITIONS ON THE FINAL PROPERTIES OF BALL BEARINGS"** completed by **BUĞRA İPEK** under the supervision of **ASSOC. PROF. DR. GÜLSÜM TOPATEŞ** and we certify that in our opinion it is fully adequate, in scope and in quality, as a thesis for degree of Master Science.

Assoc. Prof. Dr. Gülsüm TOPATEŞ

Supervisor

Ass. Prof. Mehmet Fatih ÖKTEM

Jury Member

Ass. Prof. Şeniz KUŞHAN AKIN

Jury Member

Prof. Dr. Sadettin ORHAN

Director

Graduate School of Natural and Applied Sciences

ETHICAL DECLARATION

I hereby declare that, in this thesis which has been prepared in accordance with the Thesis Writing Manual of Graduate School of Natural and Applied Science,

- All data, information and documents are obtained in framework of academic and ethical rules,
- All information, documents and assessments are presented in accordance with scientific ethics and morals.
- All the materials that have been utilized are fully cited and referenced,
- No change has been made on the utilized materials,
- All the works presented original, and in any contrary case of above statements, I accept to renounce all my legal rights.

Date: 27.10.2021 **Signature:**

Name & Surname: Buğra İPEK

ACKNOWLEDGMENTS

Firstly, I would like to express my sincere gratitude and thanks to my advisor, Assoc. Prof. Dr. Gülsüm TOPATEŞ, for her support, kindly advice, and guidance throughout my studies.

Also, I would like to express greatest appreciation to Nedim Özgür ENGİN for his patience, inspiring perspective, crucial recommendations, and all support.

I would like to express gratitude to my managers, Mustafa Faik KARAARSLAN and Dr.-Ing Feridun ÖZHAN at ORS Bearings Inc. for their guidance and support. I would like to thank my colleagues, İsmail TUNALI and Metallurgical Laboratory staff for their assistance, encourage and support.

I would like to express deepest gratitude to my parents, Erdal İPEK, Gülşen İPEK and my sister Ezgi İPEK for their love, support, and guidance throughout my life.

2021, November **Buğra İPEK**

EFFECT OF TEMPERING CONDITIONS ON THE FINAL PROPERTIES OF THE BALL BEARINGS

ABSTRACT

The primary assignment of bearing is that the machine element we can encounter in every field. It provides minimum friction between raceways of inner and outer ring with relative rotary motion and ensure smooth load transformation. The bearing must have high hardness and strength properties for resistance to external forces. The hardness of steel is dependent on carbon contents in chemical composition. For this reason, 100Cr6 bearing steel, which is defined as high carbon low alloy steel, is commonly used by bearing manufacturers. The through-hardening process consists of quenching and tempering conditions. Austenitization temperature is used at 850°C. Moreover, the quenching condition that provides high hardness, includes stress. Tempering was carried out between 150-300°C by applying 10°C intervals. Also, two different tempering durations were selected; 90 and 240 minutes. The tempering condition removes residual stress and retained austenite. Retained austenite can be decomposed into the martensite phase depending on tempering temperatures and durations. However, this case causes dimensional distortion for rings. Balls are trapped between inner and outer rings. This situation causes failure of bearing. A dimensional stabilization test should be applied to the bearing rings to observe dimensional distortion. Accordingly, tempering temperatures are determined. Since there is no international dimensional stabilization test standard, the bearing manufacturers develop their own dimensional stabilization test parameters. Three different dimensional stabilization test conditions were applied to rings according to heat classes. In this study, 6208 types of bearing rings are used. Effects of tempering conditions on the final properties of bearing rings are examined. For outer rings; hardness values were observed between 790 HV1 to 643 HV1 for 90 minutes and 775 HV1 to 658 HV1 for 240 minutes duration at 150 and 300°C tempering temperature. The amount of retained austenite was completely decomposed into martensite at 230°C for 90 minutes and 220°C for 240 minutes duration. For inner rings under the same tempering temperatures; hardness values were observed between 792 HV1 to 643 HV1 for 90 minutes and 773 HV1 and 632 HV1 for 240 minutes duration. The amount of

retained austenite was completely decomposed into martensite at 230°C for 90 minutes and 210°C for 240 minutes duration. The amount of retained austenite caused the dimensional distortion on rings according to dimensional stabilization test. The 240 minutes tempering duration is more suitable than 90 minutes for the phase stabilization of rings.

Keywords: Tempering Conditions, Retained Austenite, Martensite, Hardness, Dimensional Stabilization

TEMPERLEME KOŞULLARININ RULMANLARIN NİHAİ ÖZELLİKLERİNE ETKİSİ

ÖZ

Her alanda karşılaşabileceğimiz bir makine elemanı olan rulmanın temel görevi, aralarında rölatif dönme hareketi olan bilya ile bilezikler arasındaki sürtünmeyi minimuma indirmek ve yük aktarımını sorunsuz şekilde sağlamaktır. Rulman kuvvete karşı direnç gösterilebilmesi için sert ve yüksek dayanıma sahip olmalıdır. Çeliğin sertlik alması kimyasal kompozisyonundaki karbon içeriğine bağlıdır. Bu nedenle yüksek karbonlu düşük alaşımlı çelik olarak tanımlanan 100Cr6 rulman çeliği ortak olarak rulman üreticileri tarafından kullanılmaktadır. Islah işlemi ani soğutma ve temperleme işlemlerinden oluşmaktadır. Östenitleme sıcaklığı 850°C olarak kullanılmıştır. Yüksek sertlik sağlayan ani soğutma işlemi kalıntı gerilimler içerir. Temperleme işlemi 150°C ve 300°C arasında on derece aralıklarla gerçekleştirilmiştir. 90 ve 240 dakika olarak iki farklı temperleme süresi seçilmiştir. Temperleme işlemi kalıntı gerilimleri yok eder ve kalıntı östenitleri martensitin içine çözer. Bu yüzden on altı farklı temperleme sıcaklığı ve iki farklı temperleme süresi kullanılmıştır. Kalıntı östenit, martenzit fazının içine sıcaklık ve süreye bağlı olarak çözünür. Bu durum bileziklerde boyutsal bozulmalara sebep olur. Rulman bilyaları, iç ve dış bilezik arasında sıkışarak rulmanın çalışamaz hale gelmesine yol açar. Boyutsal bozulmayı önlemek için rulman bileziklerine boyutsal stabilizasyon testi uygulanmalıdır. Uluslararası boyutsal stabilizasyon test standardı bulunmadığından her rulman üreticisi boyutsal stabilizasyon test parametrelerini kendi geliştirmektedir. Bileziklere ısı sınıflarına göre üç farklı boyutsal stabilizasyon testi uygulanmıştır. Bu çalışmada 6208 tip rulman bilezikleri kullanılmıştır. Temperleme koşullarının rulman bileziklerinin nihai özellikleri üzerindeki etkileri incelenmiştir. Dış bilezikler için; 150 ve 300 °C tavlama sıcaklığında 90 dakika temperleme süresiyle 790 HV1 ile 643 HV1 arasında ve 240 dakika temperleme süresiyle 775 HV1 ile 658 HV1 arasında sertlik değerleri gözlemlenmiştir. Tutulan östenit miktarı, 230 °C'de 90 dakika ve 220 °C'de 240 dakika temperleme süresiyle tamamen martensite ayrışmıştır. Aynı temperleme sıcaklıklarında iç bilezikler için; 90 dakika temperleme süresiye 792 HV1 ile 643 HV1 arasında ve 240 dakika temperleme süresiyle 773 HV1 ile 632 HV1 arasında sertlik

değerleri gözlemlenmiştir. Tutulan östenit miktarı 230°C'de 90 dakika ve 210°C'de 240 dakika temperleme süresiyle tamamen martensite ayrışmıştır. Tutulan östenit miktarı, boyutsal stabilizasyon testine göre bileziklerde boyutsal bozulmaya neden olmuştur. Bileziklerin homojenizasyonu için 240 dakikalık tavlama süresi 90 dakikadan daha uygundur.

Anahtar Kelimeler: Temperleme Koşulları, Kalıntı Östenit, Martenzit, Boyutsal Stabilizasyon

CONTENTS

LIST OF TABLES

LIST OF FIGURES

NOMENCLATURE

Ac3: Upper critical temperature in hypoeutectoid alloys

Acm: Upper critical temperature in hypereutectoid alloys

c: Former treatment constant

d: Grain size of sample

Fe_3C: Cementite phase

HRC: Hardness Rockwell C

HV1: Hardness Vickers (1kg load)

l_i: Initial dimension

l_f: Final dimension

Ms: Martensite start temperature

Nital: Nitric acid and ethyl alcohol solution

T_γ: Austenitization temperature

Tp: Tempering parameter

Tt: Tempering temperature

XRD: X-Ray Diffraction

α: Ferrite phase

ε: Epsilon carbide phase

γ_R: Retained austenite phase

σ: Stress of samples

σ_0: Resistance to dislocation movement

CHAPTER 1

INTRODUCTION

1.1 Ball Bearings and Components

Bearing is a machine element that aids the rotation of objects. The purpose of the bearings is to minimize the friction between two elements with relative rotational motion. Thus, they provide smooth load transfer between machine elements. The term bearing is derived from the verb to bear [1]; a bearing is a machine element that allows one part to bear (i.e., to support) another. Around the year 1500, the first handmade drawings of ball bearings were known to be incorporated for a helicopter design by Leonardo da Vinci. However, the first sketches of roller and thrust bearings were published by Agostino Ramelli [2]. Due to the balls or rollers which scrape against each other, bearings have additional friction. The cage, which was used in bearings, was invented by Galileo in the 17th century. British inventor Philip Vaughan took the first ball bearing patent in the industrial era in 1794. This invention consists of the first modern ball bearing design [3]. A bearing may have to carry heavy static conditions as well as cyclic loads while serving credibility in arduous environments. In the Industrial Revolution, bearings have played a pioneering role, leading to the efficient operation of the new industrial machines. Steels that are proper in the complex conditions represent the material of choice in the manufacture of bearings in their many forms. In 1901, the metallurgy of the commonly used 100Cr6 (AISI 52100) on the ball bearing steel was identified by Richards Stribeck [4]. A bearing consists of five main parts: inner and outer ring, rolling element(balls), cage, and seal. Rings provide load carrying between the rotational movement of rolling elements and rings. Needless to say, they must be durable to external forces. Furthermore, the balls that are rotational parts in the raceways provide maximum performance with minimum friction. Also, the cage which grips the balls in a suitable relative position prevents the balls from contacting each other during rotation. Finally, the seal blocks the lubricant trickle from the bearing and prevents contamination arising from external influences. Bearings are classified according to high-speed applications and load-carrying

capacity. These are ball bearings and roller bearings. Ball bearings have the highest speed limit of all bearing types. The spherical structure of the balls provides minimum contact to the surface of rings. In the ball bearings, only the top point of the balls contacts with the rings.

On the other hand, roller bearings have an excellent load-carrying limit. The cylindrical or conical structures of rollers have maximum contact with the surface of rings. It has to be underlined that the bearings must have superior mechanical properties in order to provide load transfer. Bearings must have high hardness and strength. The working environment, working temperature, and hardness are significant parameters in the bearing selection. The working environment is related to pollution, dust, and scraps. The working temperature affects hardness directly. When the working temperature increases, rings must be tempered by a higher temperature. Consequently, the hardness value decreases.

The bearings are classified according to their working temperature. Heat classification of bearings is given in Table 1.1.

Table 1.1 Heat classification of bearings in ORS Bearing Company

Heat Class	SN	S0	S1	S2	S3	S4
Working Temperature	120°C	150°C	200°C	250°C	300°C	350°C
Hardness (HRC)	62-65	62±2	59±2	57±2	53±2	52±2

Figure 1.1 Type of 6208 ball bearing

Table 1.2 Type of 6208 ball bearing identification

Bearing Type	Outer Diameter (mm)	Inner Diameter (mm)	Ball Diameter (mm)	Load Carrying Capacity (MPa)(ISO76)	Speed Limit (rev./min.)
6208	80	40	18	4200	9300

The bearing rings with type number 6208 mentioned were examined during the study. The type of 6208 bearing Figure and information are given in Figure 1.1 and Table 1.2.

1.2 Bearing Steel 100Cr6(AISI 52100)

Steels are known metal alloys that contain less than 2 wt.% carbon contents. They consist of three main groups in accordance with the carbon percentage. The low carbon steel is up to 0.30 wt.% carbon content. The medium carbon steel contains between 0.30 wt.% to 0.60 wt.% carbon content. Finally, high-carbon steel consists of more than 0.60 wt.% carbon [4] in Figure 1.2. The steels are classified according to their chemical composition, such as low alloy and high alloy steel.

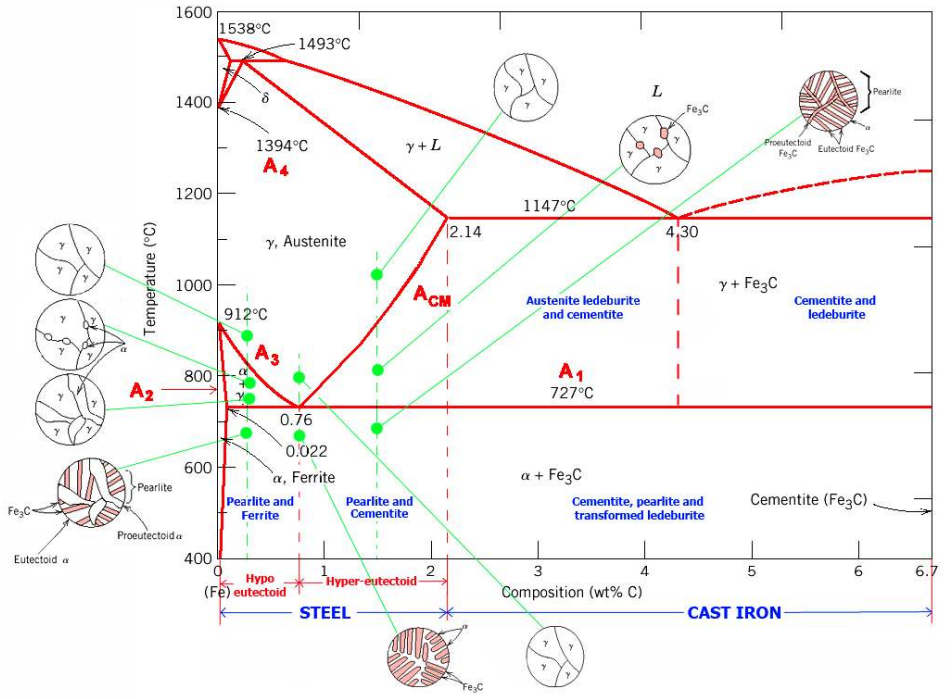

Figure 1.2 The Iron-Carbon phase diagram [5]

The bearing steel(100Cr6) is in a low alloy high carbon steel class. It includes 1 wt.% carbon and 1.5 wt.% chromium. The chemical composition of the used bearing steel is given Table 2.1. Carbon contents provide desired hardness, and chromium content improves its strength.

We have to acknowledge that alloy elements are effective factors for the formation of graphs. Boundaries of graphs can be shifted to the right side and left side to alloy elements amount (Figure 1.3). 100Cr6 can be made martensitic structure by quenching process in salt or oil bath. Mostly austenite phase is transformed to the martensite and retained austenite.

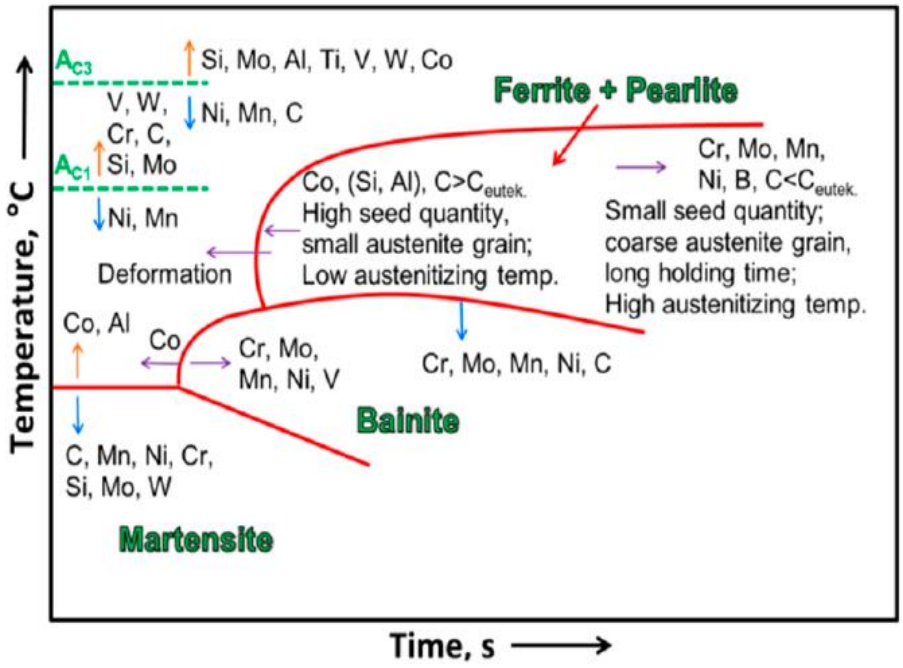

Figure 1.3 Influence of alloying, thermomechanical factors, and structure state on transformation kinetics [6]

The hardening process, which consists of the quenching and tempering process, is applied to the 100Cr6 samples. The quenching process depends on temperature and duration. It provides observations of different phases in Figure 1.3.

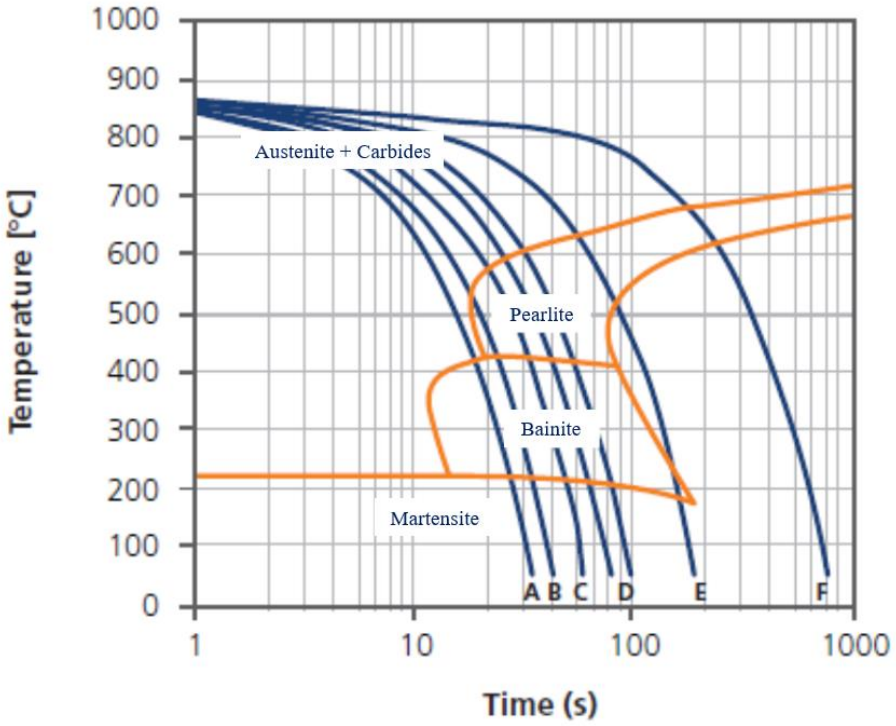

Figure 1.4 Continuous cooling transformation (CCT) diagram of the 100Cr6 steel [6]

100Cr6 steel is heated up to austenitization temperature. Different phases occur according to the cooling rate. If the cooling time is fast, the austenite phase is transformed into the martensite phase. Martensite phase is defined as the hardest phase in Figure 1.4. The martensite transformation, which is called diffusion-less, depends on the cooling rate. When the cooling rate is lower, the austenite phase is transformed to the bainite phase. It has a lower hardness value than that of the martensite phase. Bearing steel must be highly resistant to load and durable for a long-time operation. These properties affect bearing performance. Mechanical properties of 100Cr6 are given in Table 1.3

Table 1.3 Mechanical, physical and thermal properties of 100Cr6 steel [7]

Properties	**Value**
Density	7.83 g/cm^3
Specific Heat Capacity 50/100°C	0.47 kJ/(kg.K)
Thermal Conductivity	40 - 45 W/m.K
Linear expansion coefficient (0-100 °C)	12.60 µm/m.K
Young's Modulus	208 GPa
Poisson's Ratio	0.30

Hot rolled bearing steel has been employed for manufacturing. This microstructure is pearlite in ambient conditions. To start with, the hardness value is not convenient to the turning process. Hence, spheroidise annealing is applied to bearing steel. As a result, the pearlite microstructure is transformed into spherical carbides which are important for the hardening process. The hardening process improves the microstructural and mechanical properties of bearing steel. Mechanical properties of bearing steels after the spheroidise annealing and through-hardening process are given in Table 1.4. It has to be reminded that bearing rings must have high hardness and strength for long service life. Tensile strength is directly proportional to the hardness value of bearing steels.

Table 1.4 Mechanical properties of the 100Cr6(AISI 52100) steel according to the heat treatment condition [7]

Steel	Condition	Hardness (HV1)	Yield Strength (MPa)	Tensile Strength (MPa)	Elongation (%)
100Cr6	Spheroidized Annealing	220 HV1	400	700	27
	Through Hardening	720	1700	2300	2

1.3 Effect of Tempering Conditions on Bearing Steel (100Cr6)

100Cr6 is the most common raw material for bearing applications. The standard heat treatment for 100Cr6 steel is used to produce a martensitic microstructure by proper quenching and following lower temperature tempering to obtain the acceptable mechanical properties necessary for bearing. The martensitic microstructure provides adequate service life due to its high strength [8]. During the tempering process, martensite is reheated at a temperature below the eutectoid line, kept for a specified duration, and air-cooled.

Tempering condition improves ductility and toughness of samples, besides removing retained austenite and residual stresses. It stabilizes the microstructure. Tempering conditions allow carbon saturated martensite to transform to tempered martensite, consisting of retained austenite, ferrite, and cementite phases. The conventional austenitization process for 100Cr6 steel is implemented at 850°C for 20 minutes. However, equilibrium cannot be adequate within 20 minutes of austenitization. Guillot who studied for optimization of the thermal treatment of a roller bearing steel reported the kinetics of cementite dissolution in bearing steel [9]. The final microstructure after the quenching process is martensite with about 10 vol. % of retained austenite [10]. The tempering condition is followed at different temperatures. When the tempering temperature increases, decomposition of the retained austenite and size of carbide particles increases. Softening occurs on bearing steel after tempering conditions.

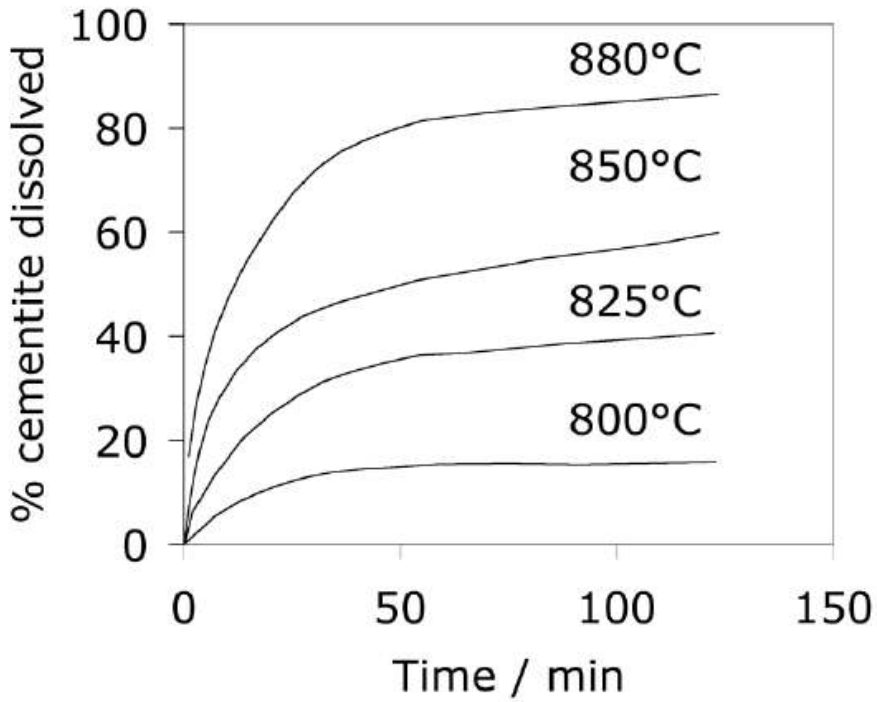

Figure 1.5 Kinetics of cementite dissolution in 100Cr6 steels, beginning with spheroidized structure, as a function of austenitization temperature [9]

1.3.1 Effect of Tempering Conditions on Retained Austenite of Bearing Steel

Bearing steels are conveniently hardened to the desired level by austenitizing at temperature nearly upper critical temperature (Ac3), quenching and tempering. The metallurgical structure is tempered martensite and retained austenite. Retained austenite is observed in quenched high carbon alloyed steels. The microstructure is a metastable phase that is decomposed under thermal or mechanical stresses. When the tempering temperature is increased up to martensite start phase (Ms), retained austenite is decomposed into martensite.

Additionally, tempering duration is a parameter of decomposition of the retained austenite. Retained austenite cannot appear after etching with 3% nital. It can be observed by XRD methods. Retained austenite can be hazardous due to size change of bearings.

Martensite is a supersaturated metastable phase retaining the parent austenite phase of carbon concentration. Martensite tempering consists of five main stages [11, 12, 13 ,14]. In this study, three stages: Stage 1, Stage 2, and Stage 3 were investigated.

Stage 1: ($100 < T < 200°C$),

$\alpha' \rightarrow \alpha'' + \varepsilon$: Oversaturated martensite rejects carbon, creating metastable nonstoichiometric epsilon carbides ($Fe_{2,4}C$).

Stage 2: ($200 < T < 300\ °C$),

$\gamma_R \rightarrow \alpha + Fe_3C$: Retained austenite is a metastable phase, decomposes into ferrite and cementite (Fe_3C).

Stage 3: ($250 < T < 350°C$),

$\alpha'' + \varepsilon \rightarrow \alpha + Fe_3C$: Carbon precipitates from weaken martensite to cementite carbides.

If tempering temperature is increased, decomposition of the retained austenite is increased. The samples expanse due to the decomposition of retained austenite. When retained austenite content is high, the sample includes a lower carbon concentration. If the tempering temperature and duration increase, decomposition of the retained austenite increases; hence carbon concentration of the sample increases. Eigenstrain is an example of decreasing function of the carbon content of retained austenite. When the initial carbon concentration of martensite increases in solid solution, dimensional balance will not deteriorate. An increase of initial carbon concentration increases the shrinkage associated with martensite, but the expansion of the carbide precipitates increases at the same time. Carbon segregation on defects only influences the expansion of Fe_3C during the precipitation.

Higher temperatures and durations provide lower retained content. For bearing steel, tempering temperatures lower than 200°C will not observe visible lowering retained austenite content [15,16].

In 1970, retained austenite content determination is possible to depend on Ms temperature and quenching time between 700 and 300°C during cooling [17].

$$\gamma = exp[-0.011(Ms - 20)(1 - \mu)]$$

$$\text{with } \mu = 0.41\left[1 - exp\left(-0.03\left(\Delta t_{300}^{700}\right)^{0.6}\right)\right] \quad (1.1)$$

This formula includes the influence of cooling rate on forms of intermediary transformation such as pearlite or bainite. The estimation of subsequent Ms and retained austenite amount is observed to transform after the intermediate phase transformation. Unfortunately, this formula cannot include intermediate quench deduction such as marquenching treatments, which submit an isothermal duration below Ms before final quenching. However, this situation increases the amount of retained austenite.

1.3.2 Effect of Tempering Conditions on Mechanical and Physical Properties of Bearing Steel

The mechanical and physical properties are essential for the service life of bearing. Hardness and working temperature are the most critical parameters for the selection of bearings. Bearings have heat stabilized classes according to the desired working temperatures in Table 1.1. When the working temperature is higher, bearing rings must be tempered at a higher temperature. Hardness of bearings decreases due to increasing working temperatures. Hence, hardness reduction causes a decreasing strength and toughness of bearings. Sample should be worked at a higher temperature.

The hardness of martensitic bearing steels is given against tempering temperature in Figure 1.6. With increasing of the austenitization temperature above 840°C does not increase the hardness of the bearing steels because the soft retained austenite content increased to be transformed during quenching in austenite carbon concentration.

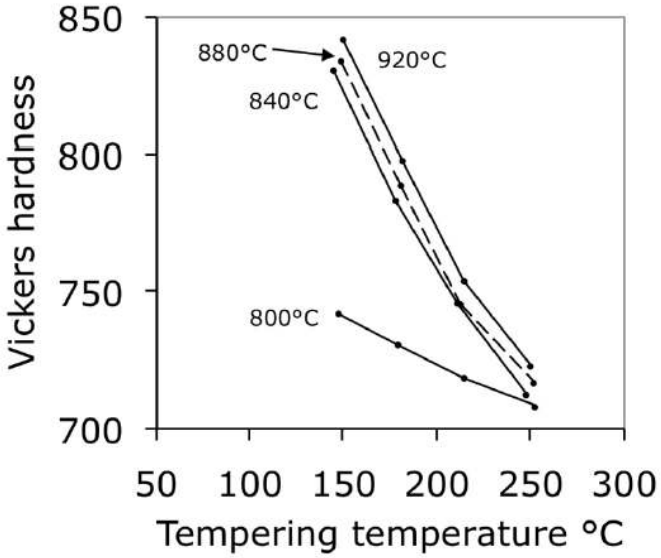

Figure 1.6 Hardness of 100Cr6 steel according to tempering and austenitization temperature [18]

Although tempering temperature is a dominant factor for tempering conditions, durations also have a strong influence. However, this situation is less examined and explored by researchers. Tempering duration should be investigated because of the effect of all tempering processes diffusion character [19,20]. With the increase of the tempering temperature, particles move faster and start to be coarser. Retained austenite decomposes into the martensite. Dimensional stability is observed at higher temperature conditions due to the retained austenite removal. The hardness of bearing reduces but heat resistance increases thanks to the higher tempering temperature applications.

According to Hollomon Jaffe and his coworkers' studies, optimal tempering conditions depend on the tempering temperature and durations. That means spending energy adequately for heating up with minimum duration. Tempering condition is related to the chemical composition of the steel. Therefore, studies should be performed according to the steel types. Hollomon Jaffe equation is defined Eq. (2) [21]:

$$Tp = T \times (c + logt) \tag{1.2}$$

Tp is tempering parameter, T is tempering temperature in K, t is tempering duration is sec. and the value of parameter c is constant according to steel types and former treatment.

Constant of c is easily calculated with the same tempering hardness value by using tempering temperature and duration Eq. (3) [21]:

$$c = (T2logt2 - T1logt1)/(T1 - T2) \quad (1.3)$$

When increasing of the tempering temperatures or durations, the tempering parameter value raises. This causes the hardness reducing.

Quenched samples include two unsuitable parameters for dimensional balance, which are residual stresses and retained austenite in the samples. Retained austenite prevents from the atomic movement of martensite. This situation is caused by internal stresses. Therefore, samples are tempered to keep a homogeneous structure. With the tempering temperature increasing, retained austenite starts to decompose into martensite. Hence residual stress and retained austenite content decrease. According to the kinetics of stress relaxation studies for bearing steels, in Figure 1.7, tempering temperature and duration remove internal stresses.

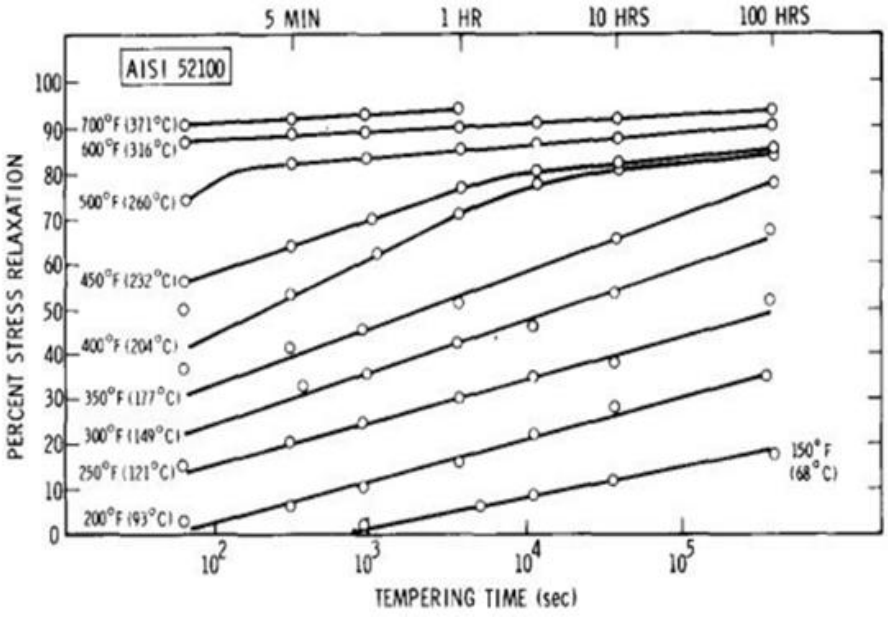

Figure 1.7 Kinetics of stress relaxation in hardened 52100 steel. Initial outer-fiber stress: 325 N/m^2 [22]

Percentage of stresses are related to retained austenite content. When the decomposition of retained austenite is completed, the stress relaxation line moves to stabilize positively.

The dimensional stability of samples directly affects the fatigue life of bearings. Therefore, a dimensional stabilization test is applied to the through-hardened samples.

Average dimension changes are measured by using Eq.4;

$$Strain\ percentage(\frac{dl}{li}\%) = \frac{Final\ dimension(lf) - initial\ dimension(li)}{initial\ dimension(li)} \times 100 \quad (1.4)$$

Initial dimension values are measured after grinding process. Final dimension values are measured after dimensional stabilization test. The dimensional change depends on many conditions. Phase transformation and precipitation occurs during the hardening process. This situation causes to the transformation strains. Tempering process provides the relaxation of samples. External stress and ambient conditions affects the working of bearings negatively. All of them causes the dimensional change. Bearing temperature and its dimensional change ratio are given in Figure 1.8.

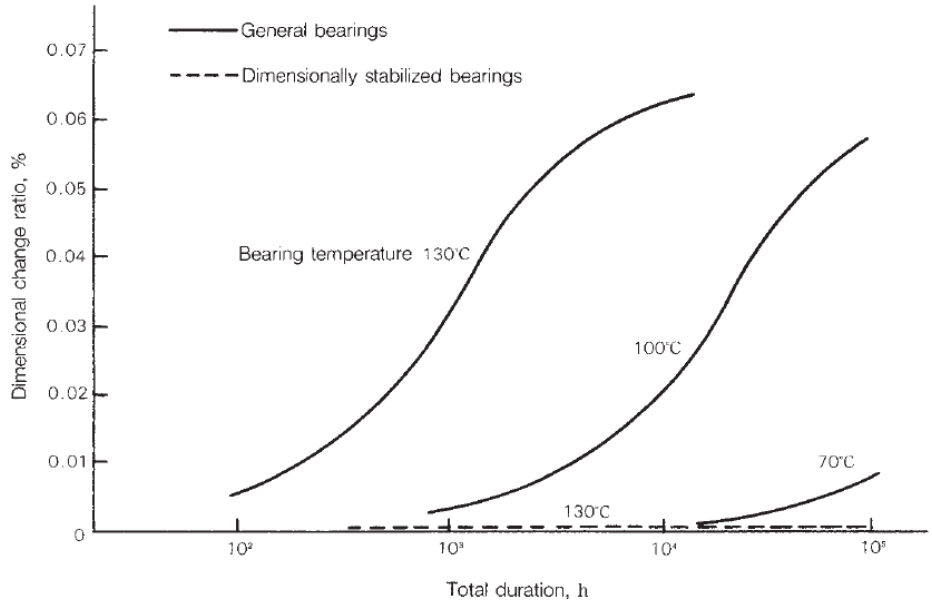

Figure 1.8 Bearing temperature against dimensional change ratio [23]

1.3.3 Effect of Tempering Conditions on Microstructure of Bearing Steel

Bearing steels consist of the ferrite and cementite phases in ambient conditions. This microstructure is not convenient for the soft grinding process. Therefore, samples are treated by a spheroidise annealing for soft grinding. The microstructure of the sample is transformed to ferrite and globular cementite. Soft grinding samples are treated through a hardening process for gaining hardenability and strength. The hardening process consists of quenching and tempering. Microstructure of sample includes martensite and retained(untransformed) austenite phase by quenching process. The martensitic microstructure has hard and brittle mechanical properties. Tempering conditions are necessary for the homogenous microstructure and balanced mechanical properties. Hardness, toughness, carbide size, and retained austenite content depend on a tempering process. After the tempering process, samples that are treated, have globular carbides into tempered martensite. With the tempering temperature increasing, retained austenite is decomposed into martensite. However, it does not appear in the microstructure. When retained austenite starts to decompose into martensite, globular carbide grains expand for being a stable phase. Samples reach homogeneous carbide grains and balanced martensite phase thanks to the expansion of the carbide grains. This situation provides dimensional stability and long service life.

Hall and Petch proved that the yield stress σ (the hardness) depends on the reciprocal square of grain(particle) size d. It follows the equation (5) [24]:

$$\sigma = \sigma_0 + kd^{-0.5} \tag{1.5}$$

where k is the measure of the local stress required to initiate plastic flow at the grain boundary, σ_0 is resistance to dislocation movement and d is the grain size of sample [25]. Surface areas of samples provide the resistance of the stress. Due to the lower tempering temperature conditions, samples have smaller particle sizes and high-stress resistance. Hence the hardness of samples is higher. If the diameter of the particle size is larger, the hardness of samples decreases due to the reduction of the surface area. Baracaldo examined the grain size and hardness relations for 0.6 wt.% C steel. The average grain size of samples was between 0.030 and 2.8 μm. Heat treatment conditions affects to the samples hardness. While, the hardest value was obtained as

720 HV1 in 0.030 μm grain size, the softest value was observed as 235HV1 in 2.8 μm grain size [53].

Tempering condition affects phase transformation, mechanical and physical properties and microstructural changes. Three main topics were examined during the experiments. There are many approaches about dimensional stabilization tests. In this thesis, dimensional stabilization test methods are preferred according to the heat classes of samples. Dimensional changes have occurred due to the different tempering conditions.

CHAPTER 2

EXPERIMENTAL METHODS

2.1 Material

1.3505 (100Cr6) steel grade was used according to DIN EN ISO 683-17 standard. Figure 2.1 shows the dimension of the type of 6208 inner ring and outer ring. Table 2.1 shows the chemical composition of the used raw material for this study.

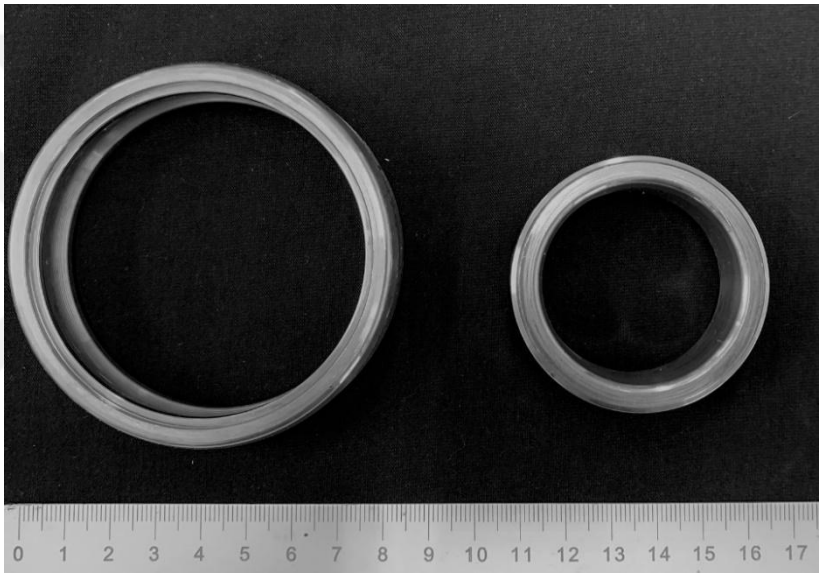

Figure 2.1 6208 inner and outer ring

Table 2.1 Chemical composition of 100Cr6 raw material used

Composition in weight (%)									
C%	Si%	Mn%	P%	S%	Cu%	Cr%	Mo%	Al%	O%
1.01	0.27	0.35	0.002	0.007	0.02	1.48	0.001	0.021	0.001

2.2 Hot Forging

Metals that are subjected to plastic deformation above their recrystallization temperature maintain their shape during the cooling. Under the ambient conditions, 100Cr6 steel bars have approximately 30 HRC hardness values. Therefore, steel bars

were heated up to 1150°C by induction machine. The effect of the applied pressure started to form as a blank shape. A forging machine (Sakamura HBP-120) was used for the hot forging process. The inner ring and outer ring were forged simultaneously.

2.3 Spheroidise Annealing

Spheroidise annealing is a process that includes controlled heating and cooling to obtain a microstructure of spherical carbides in a ferrite matrix. After forging, the hardness of the blanks was not suitable for turning. So, spheroidise annealing was applied to the blanks to facilitate turning. Blanks were heated up to 790 °C and then cooled gradually down to 690 °C for approximately 16 hours as a standard process. Spheroidise annealing graph is given in Figure 2.2. A Roller conveyor furnace (Aichelin 203) was used during the spheroidise annealing process.

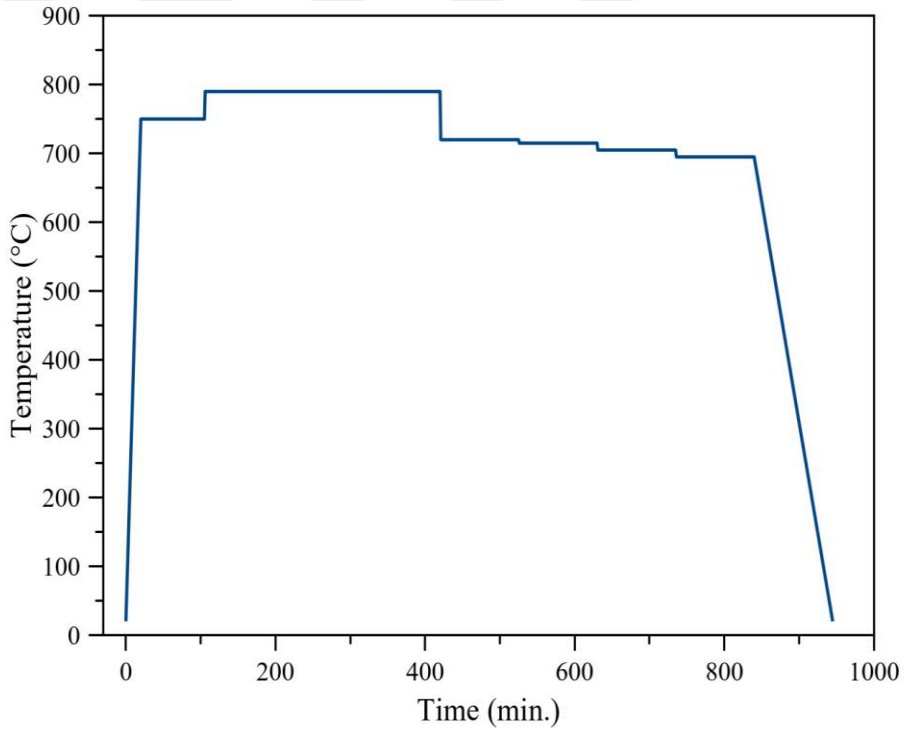

Figure 2.2 Spheroidise annealing graph

2.4 Through Hardening (Quenching and Tempering)

Through hardening is a heat treatment process to obtain desired hardness, strength, and toughness of rings. Rings were heated up to austenitization temperature (850°C) and

were hold 45 minutes for homogenous phase distribution. After, samples were immersed to oil or salt bath for 15 seconds as a cooling mechanism to ensure hardness. This step is called quenching process. Roller conveyor furnace (Aichelin 20 014 with oil quenching furnace) for inner rings and (Aichelin 20 018 with salt quenching furnace) for outer rings were used during the quenching process. Then, samples are tempered. 16 different tempering groups between 150-300°C were used. Each group was contained 90 and 240 minutes of tempering durations. Quenching and tempering process named as through hardening is given in Figure 2.3. During the study, type of 6208 rings were used and through-hardening was applied to 192 inner rings and 192 outer rings. Quenching process parameters were preferred constant. However, tempering processes parameters were varied. Each group has twelve inner rings and twelve outer rings. Rings were classified according to rings' tempering temperatures and durations.

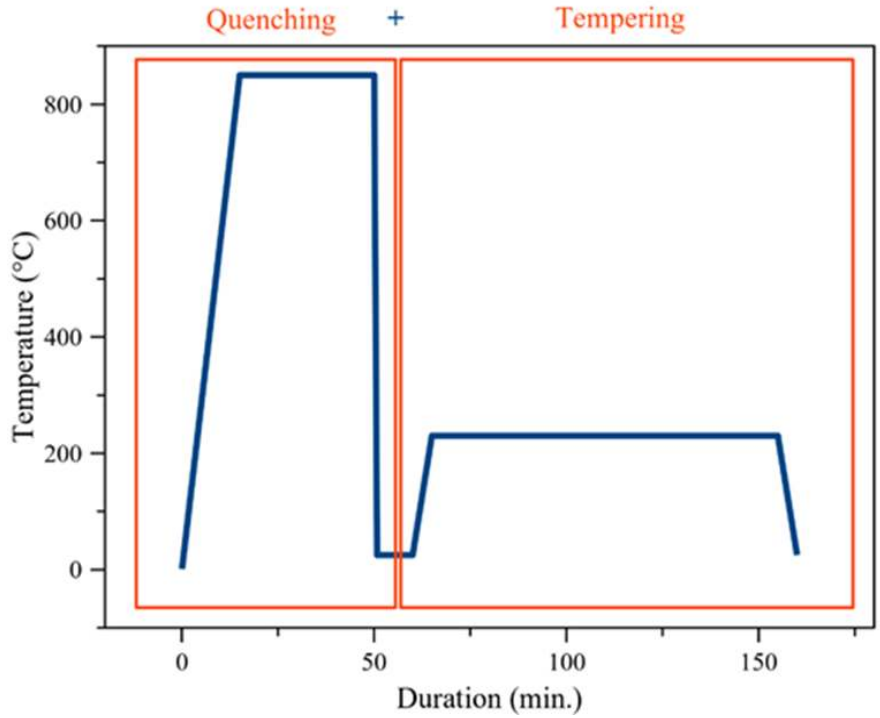

Figure 2.3 Through Hardening graph

Figure 2.4 Oil Quenching Furnace (20 014) for through hardening of inner rings

Figure 2.5 Salt Quenching Furnace (20 018) for through hardening of outer rings

Roller hearth oil quenching furnace and roller hearth salt quenching furnace were used during the heat treatment conditions. Maximum furnace temperatures and operation temperatures are same. The main differences between these furnaces are bath temperatures and quenching rate. While oil bath temperature is 160°C, salt bath temperature 215°C. Samples washes after oil and salt bath for solution elimination. Properties of the furnaces are given in Table 2.2.

Table 2.2 Quenching Process Parameters

Properties	**Oil Quenching Furnace (20 018)**	**Salt Quenching Furnace (20 014)**
Furnace temperature max. (°C)	900	900
Operation temperature (°C)	850	850
Bath temperature (°C)	160	215
Quenching rate (°C/sec.)	80	85
Protective Gas	Nitrogen (N_2) and Propane (C_3H_8)	Nitrogen (N_2) and Propane (C_3H_8)

Sample denomination was defined according to tempering temperatures and durations. Rings classification is given in the Table 2.3 as an example of sample denomination. For example, T150-I/O1; T150 refers to tempering temperatures and I/O1 refers to 90 minutes and I/O2 refers to 240 minutes tempering duration for inner and outer rings. The sample denomination changes at 10°C intervals according to applied tempering temperature.

Table 2.3 Example of heat treatment conditions and sample denominations in this study

Sample Denomination	Quenching Temperature / Duration (°C/min.)	Tempering Temperature (°C)	Duration (min.)
T150-I/O1	850	150	90
T150-I/O2	850	150	240

2.4.1 Tempering

Tempering was carried out between 150-300°C by applying 10°C intervals. Also, two different tempering durations were selected; 90 and 240 minutes. Each tempering condition was applied for six inner and six outer rings. After the tempering process, one representative sample was randomly selected from inner and outer rings for hardness and retained austenite measurements.

A chamber type (Aichelin Tempering 1) furnace was used for all tempering processes for both rings.

Figure 2.6 Aichelin tempering furnace for both types of rings

Properties of tempering furnace are given in Table 2.4.

Table 2.4 Properties of Aichelin tempering furnace

Properties	Aichelin Tempering Furnace
Furnace Temperature Ranges (°C)	300 - 700
Operation Temperature Ranges (°C)	150 - 300
Maximum Charge Capacity (kg)	650

2.5 Grinding

Grinding is the process of removing metal particles from hard material to obtain final dimensions. The grinding process of outer rings consists of hard face grinding, hard outer diameter grinding, raceway grinding, and raceway superfinishing. A grinding machine (Koyo) for hard face grinding and hard outer diameter grinding, (Toyo T157) for raceway grinding, and (Daisei 2BG) for raceway superfinishing were used for outer rings. The grinding process of inner rings consists of hard face grinding, raceway grinding, bore grinding, and raceway superfinishing were applied to inner rings. Grinding machine (Koyo) for hard face grinding, (Toyo T235) for raceway grinding, (Toyo T117) for bore grinding, and (Daisei 2BG) for raceway superfinishing were used for inner ring grinding.

2.6 Dimensional Measurement

After the grinding process, all samples were labeled according to tempering temperature and durations. Outer diameter was measured from the top, middle, and bottom sides for outer rings. Bore diameter was measured from the top, middle, bottom sides for inner rings. The same measurements were composed again after the dimensional stabilization test. Rings were held for one hour for suitable measurement conditions in the metrology laboratory. Diameters were measured mechanically from each ring's top, middle and bottom points by measurement device (Pratt & Whitney LMU175) (Figure 2.7).

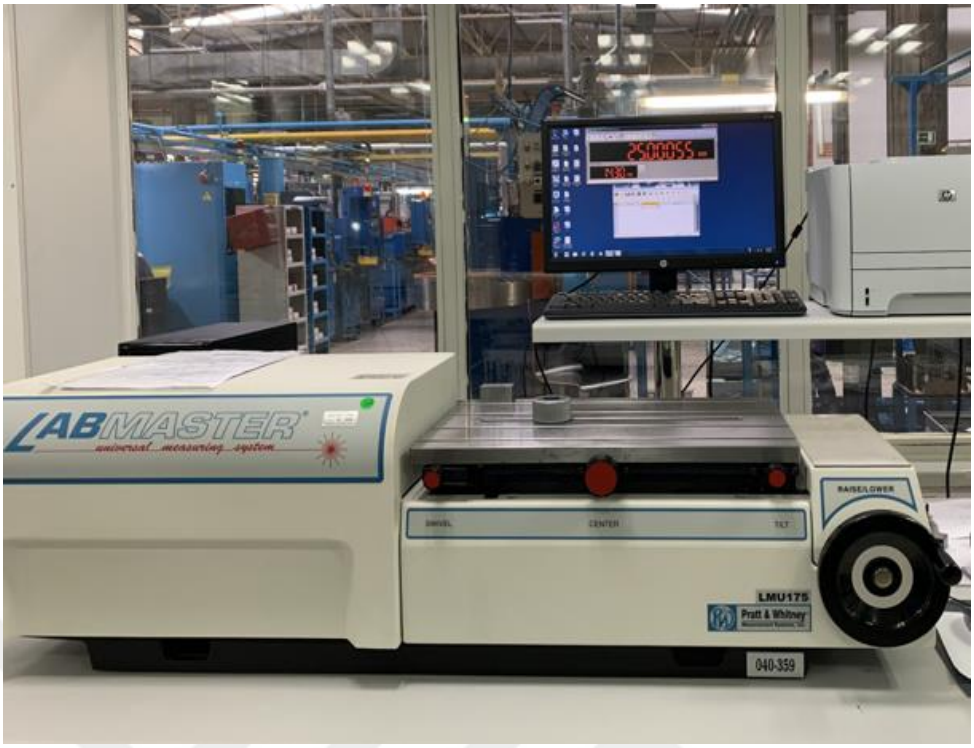

Figure 2.7 Diameter measurement instrument

Measurement technical information is shown in Table 2.5.

Table 2.5 Technical details about measurement instrument

Properties	**Measurement Instrument (LMU175)**
Instrument Uncertainty (µm)	0.05+ 5L/1000 (±2 std. dev.)
Repeatability (µm)	0.04 (±2 std. dev.)
Resolution (µm)	0.0025
Measurement Range (mm)	Internal:0.5 to 356, External: 0 to 330
Standard Contact Force (N)	0.14

2.7 Dimensional Stabilization Test

A Dimensional test was performed to rings according to tempering temperature groups for dimensional stability. Samples consist of ORS heat treatment classes: S0, S1, and

S2. Dimensional stabilization temperatures were determined in conformity with the heat treatment classes. Test parameters are given in Table 2.6 in detail.

Table 2.6 Dimensional stabilization test parameters

	Heat Treatment Classes (ORS)	**Dimensional Stabilization Test Temperature (°C) / Duration (hour)**
T150 - T220	S0	235 / 4
T230 - T280	S1	245 / 4
T290 - T300	S2	300 / 4

2.8 Microstructural Examination

Metallographic preparations were applied before the microstructural examination. First of all, samples were cut in longitudinal sections, and then samples were mounted with bakelite. After that, samples were ground with 100, 240, 600, and 1200 grids of sandpaper. They were polished with 3µm diamond paste. Finally, a smooth surface was obtained and samples were etched by 3 vol. % nitric acid and 97 vol. % ethyl alcohol solution. The distribution of carbides was examined by Scanning Electron Microscope (HITACHI SU 5000) (Figure 2.8).

Figure 2.8 Scanning Electron Microscope

The Scanning Electron Microscope at an acceleration voltage of 20kV was used during the SEM examination. Tempered samples were examined by SEM according to the change of tempering temperatures and durations. All of the examined samples were etched with 3% nitric acid and 97 % ethyl alcohol solution.

2.9 Hardness Measurement

All samples were measured before and after the tempering process. Hardness values of rings were measured from five points on surface. The mean value of the results was recorded after the tempering process. Vickers microhardness test machine (KB-30S) was used. One kilo-gram force was loaded to rings for fifteen seconds. Measurements were performed in accordance with standard ISO 6507-1. The hardness test device is given in Figure 2.9.

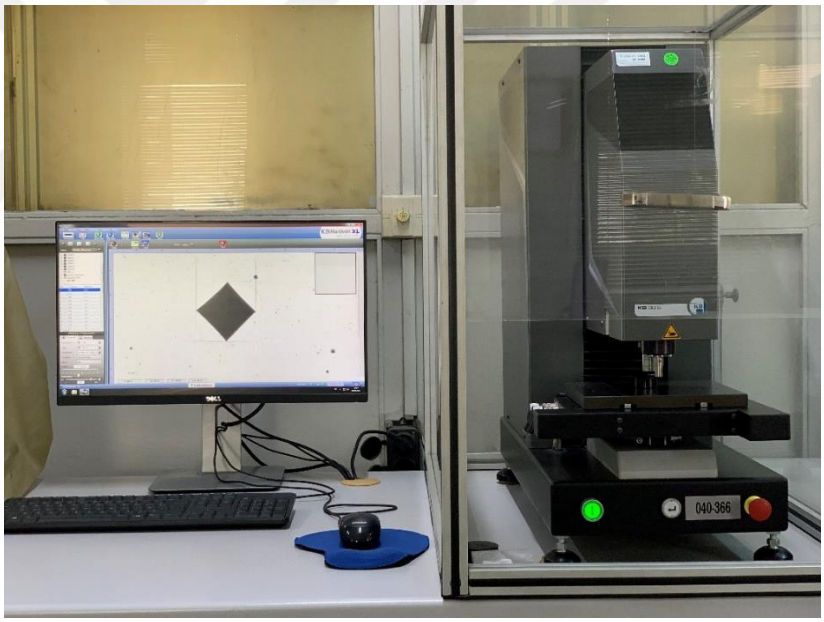

Figure 2.9 Vickers microhardness test machine

2.10 Retained Austenite Measurement

Retained austenite content was analyzed by Seifert XRD 3003 PTS for tempered rings. As seen in Figure 2.10, this system consists of three main parts: goniometer, X-Ray detector, and X-Ray generator tube. Measurement parameters are given in Table 2.7. The amount of retained austenite was measured from T150 to T240 samples.

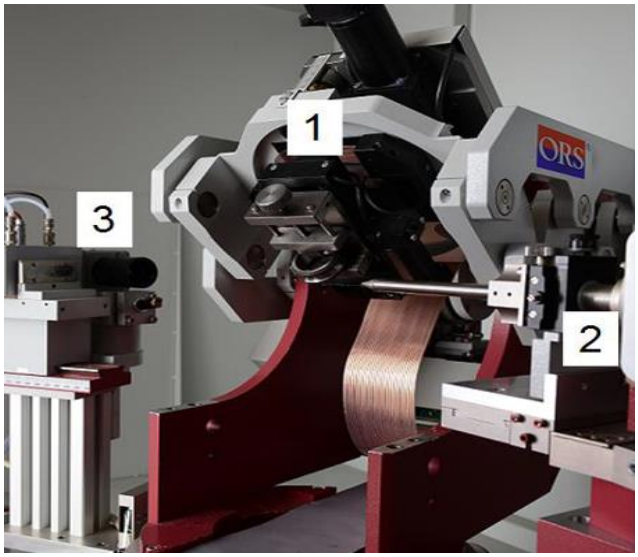

Figure 2.10 X-Ray Diffractometer (XRD), Seifert 3003 PTS. (1) Goniometer, (2) X-Ray Generator Tube and (3) Position Sensitive Detector

Table 2.7 XRD measurement parameters

Parameters	**Seifert XRD 3003 PTS**
Collimator (mm)	3
Number of Scans	4
Scan Ranges (°)	102.00-168.00
Step With	0.02
Time (s)	300
Scan Axis	2:1 Absolute
Scan Mode	Step-scan

2.11 Image Analyzing Technique (ImageJ)

One ring is prepared from each tempered group for microstructural examination. In order to calculate the particle size and fraction area of carbides, one image at a magnification of 500x is taken from each group by using a light optical microscope.

Then 50x50 μm are cut from each image. The fraction area and particle size of carbides are computed by the ImageJ image processing software.

CHAPTER 3

RESULTS AND DISCUSSIONS

3.1 Effect of Tempering Temperature on Retained Austenite

Retained austenite is a noteworthy phase on a martensitic microstructure which is based on prevalent bearing steels. Retained austenite phase leads to dimensional instability on bearing rings. The presence of retained austenite, heating the shaft before the bearing is mounted, increasing the heat of the bearing under mechanical loads, and the bearing's exposure to a temperature above the operating temperature cause the retained austenite to dissolve, and the dimensional change occurs. These reasons cause the failure of the bearing.

Changes in retained austenite contents for outer and inner rings against tempering temperature and times are presented in Figures 3.1 and 3.2. For outer rings, the retained austenite content was 11.8% at 150°C. Retained austenite decomposition was performed in high amount at 180°C. Stage 1 tempering provides high hardness due to the e-carbide phase. It prevents the decomposition of the retained austenite at low tempering conditions. The decomposition rate of retained austenite was high; between 180 and 230 °C tempering conditions. Stage 2 tempering all excess carbide particles precipitate and transform to the more stable cementite phase. With the increasing of tempering temperature, retained austenite contents were reduced. It was observed that retained austenite was completely decomposed into martensite at 230°C tempering temperature for 90 minutes.

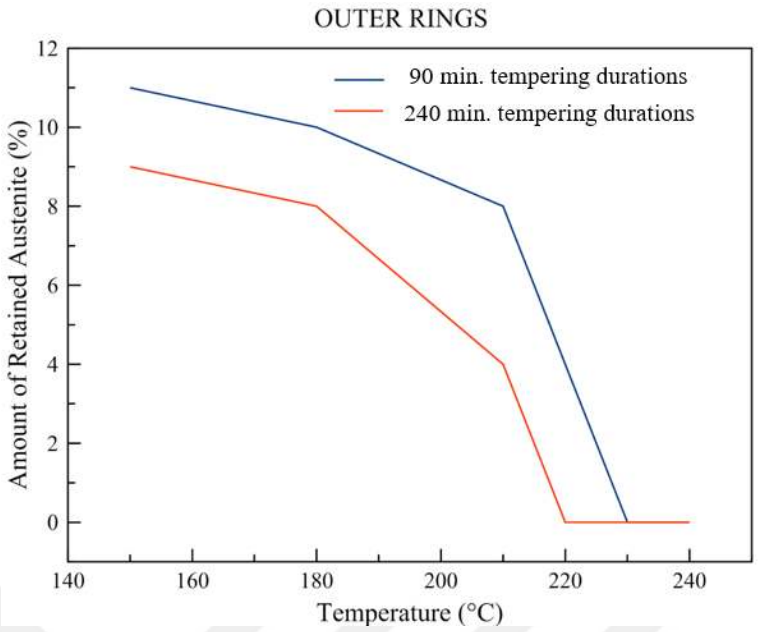

Figure 3.1 Amount of retained austenite against tempering temperature for outer rings

For inner rings, the retained austenite contents were 10% at 150°C and 8% at 180°C. With the increasing of tempering temperature, retained austenite contents were reduced, and it was entirely decomposed into martensite at 230°C for 90 minutes.

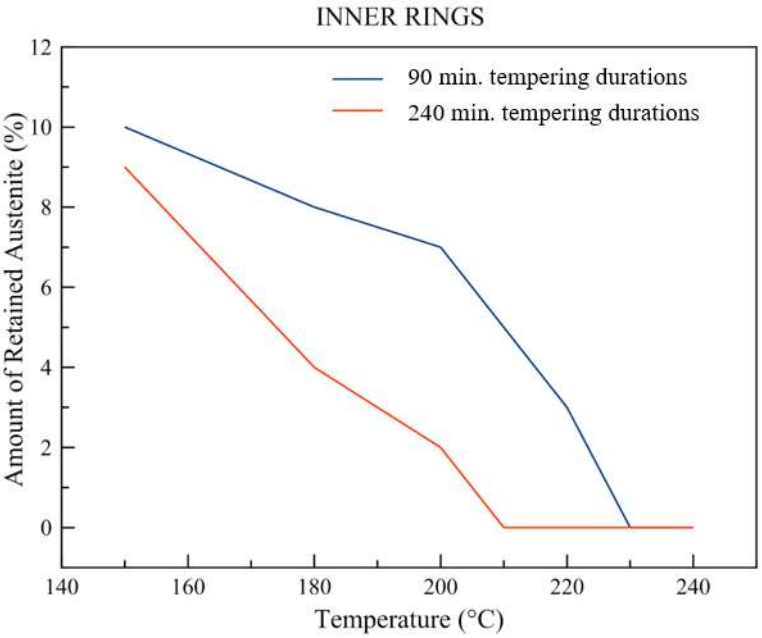

Figure 3.2 Amount of retained austenite against tempering temperature for inner rings

Even the outer and inner rings have similar cross-sectional areas. The diameter of the outer ones is two times larger than that of the inner ones. When the diameter of rings was increased, distortion may be observed during the quenching process due to the aspect ratio. Quenching solution (salt or oil), which is contacted to the surface of the rings, is led to distortion due to the heat contact effect. This situation can be explained by retained austenite phase, which confined the expansion of the carbide particle size. The intensity of distortion is related to retained austenite content. Therefore, decomposition of retained austenite was completed at 210°C for inner rings, where for outer rings, it continued to 220°C for 240 minutes.

In hypereutectoid steels, the amount of the retained austenite changes with the austenitization temperature (Tγ), which is below the upper critical temperature in hypereutectoid alloys (Acm) temperature of the alloy. Tγ is not the only parameter that determines the carbon concentration of austenite. The dissolution rate of carbides also depends on the grain size distribution of the spheroidized carbide in the microstructure before heating. These factors affect the amount of retained austenite during quenching [26].

The retained austenite decomposition caused dimensional instability during the use of bearing; therefore, the amount of retained austenite should be minimized by suitable tempering conditions. The tempering process consists of three stages. In stage 1, the tempering temperature (T_t) is less than 200°C, and at this temperature solid phase forms e-carbide having more carbon clusters. In stage 2, T_t is between 200°C to 300 °C; all excess carbon precipitates and transforms into a more stable cementite structure. In stage 3, T_t is between 200°C to 350 °C; carbides become coarsen.

Additionally, dislocation recovery and recrystallization of ferrite plates into coaxial grains are observed. The retained austenite can entirely be decomposed with proper austenitization or tempering conditions in bearing rings. Tempering leads to a dramatic reduction in the decomposition of retained austenite. The partitioning of carbon from the retained austenite into martensite provides a more stable supersaturated martensite phase [27].

Tempering treatment reduces micro-stresses and provides dimensional stability with the decomposed retained austenite. This situation is another interpretation for the influence of tempering on the stability of the retained austenite.

In Figure 1.7, when the tempering temperature was 150°C, retained austenite prevented stress relaxation of the bearing steel sample. Therefore, stress relaxation was approximately 20%. Due to the amount of retained austenite it was nearly 12% the stress relaxation percentage was low. For 230°C, the retained austenite was completely decomposed into martensite, and the stress value was observed to increase to 60%. For 300°C, homogenization of carbide particles was provided thoroughly, and the stress relaxation was observed to reach up to 80%. Stresses cannot readily be relieved without heat treatment that promotes long-range atomic diffusion over long distances. Split rings that are elastically stressed by inserting wedges into the split led to stresses [22]. These stresses were reduced by tempering temperatures and duration on bearing steel.

3.2 Effect of Tempering Duration on Retained Austenite

Two different tempering durations, 90 and 240 minutes were selected to investigate their effects on final properties. For outer and inner rings, complete dissolution of retained austenite was obtained at lower temperatures for 240 minutes. The retained austenite was consumed at 230°C in 90 minutes for outer and inner rings, while in 240 minutes, this reduced to 210 and 220°C, respectively (Figure 3.2).

Inner rings were able to dissolve the retained austenite at a lower temperature in 240 minutes. As can be seen from the results, the contents of retained austenite were consumed by increasing the tempering durations at lower temperatures, and microstructural homogenization and dimensional stabilization were ensured all over the ring.

Martensitic transformation is a diffusion-less phase transformation that was composed of atomic motions. Since longer tempering duration was easily provided homogenization of samples.

Previous studies (Figure 1.7) observed that the stress percentages of samples tempered between 150 and 230°C decreased as the tempering duration increased. However, duration did not affect the stresses of rings for higher than 260°C tempering temperatures. When the tempering temperature was above the Ms, retained austenite was entirely decomposed into martensite. Due to the decomposition of retained austenite, stress relaxation and microstructural homogenization were provided in a short time. According to the Hollomon Jaffe equation, the changes of tempering parameter (Tp) depend on tempering temperature and duration.

3.3 Effect of Tempering Temperature on Mechanical and Physical Properties

Similar mechanical values can be obtained with a lower tempering temperature and longer tempering duration or higher tempering temperature and shorter tempering duration. Tp is validated up to 500°C tempering temperatures. When the tempering temperature and duration increase, Tp decreases. This situation leads to reduce the resistance of the material to external forces. During the experiment, the austenitization temperature is selected at 850°C, and the cooling rate is set at 15°C/s. Therefore, martensitic microstructure is obtained. Quenched samples are hard and brittle. They must be tempered for gaining strength. Tempering has a positive effect on the fatigue life of bearings. Hardness values of outer and inner rings tempered between 150°C - 300°C are given in Figures 3.3 and 3.4. The hardness value continuously decreased as the tempering temperature was increased. When the outer rings were examined, the value was measured as 790 HV1 at 150°C, it decreased to 756 HV1 at 180°C. Decomposition of retained austenite and formation of coarser carbide particles reduced hardness to 717 HV1 at 230° according to the 90 minutes tempering duration. The hardness reduced to 658 HV1 at 300°C tempered rings.

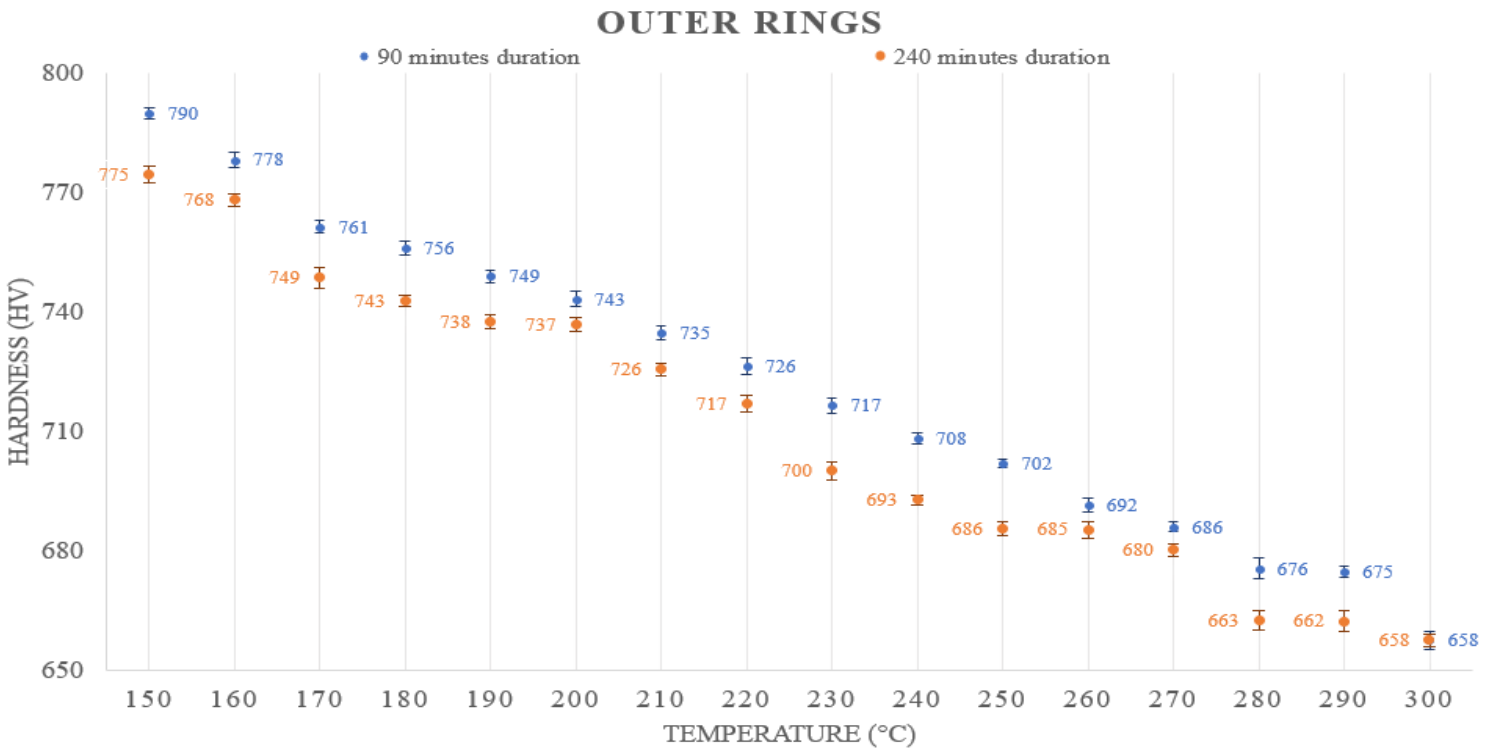

Figure 3.3 Hardness against tempering temperature for outer rings

When the inner rings were examined, similar results were obtained. The reason for this, both rings had the same width and thickness. The hardness value was 792 HV1 at 150°C. It rapidly decreased between 150 and 180°C due to the decomposition of retained austenite in a higher amount. In stage 1, tempering led to the formation of e-carbide that has more carbon clusters which provided high resistance against the external stresses. Tp depended on temperature and duration. A low Tp value means high resistance to the external forces. The hardness value decreased slowly between 190 and 240°C. Due to stage 2 tempering, all excess carbide precipitated and transformed into a more stable cementite structure. Carbide particles started to coarsen, and they aligned homogeneously. Decomposition of retained austenite completed at 230 °C and hardness drop occurred in less amount between 250 and 280 °C. The hardness decreased to 643 HV1 at 300°C. In stage 3 tempering, recrystallization of ferrite plates started to be observed into coaxial grains, which leads to reduce the hardness fast.

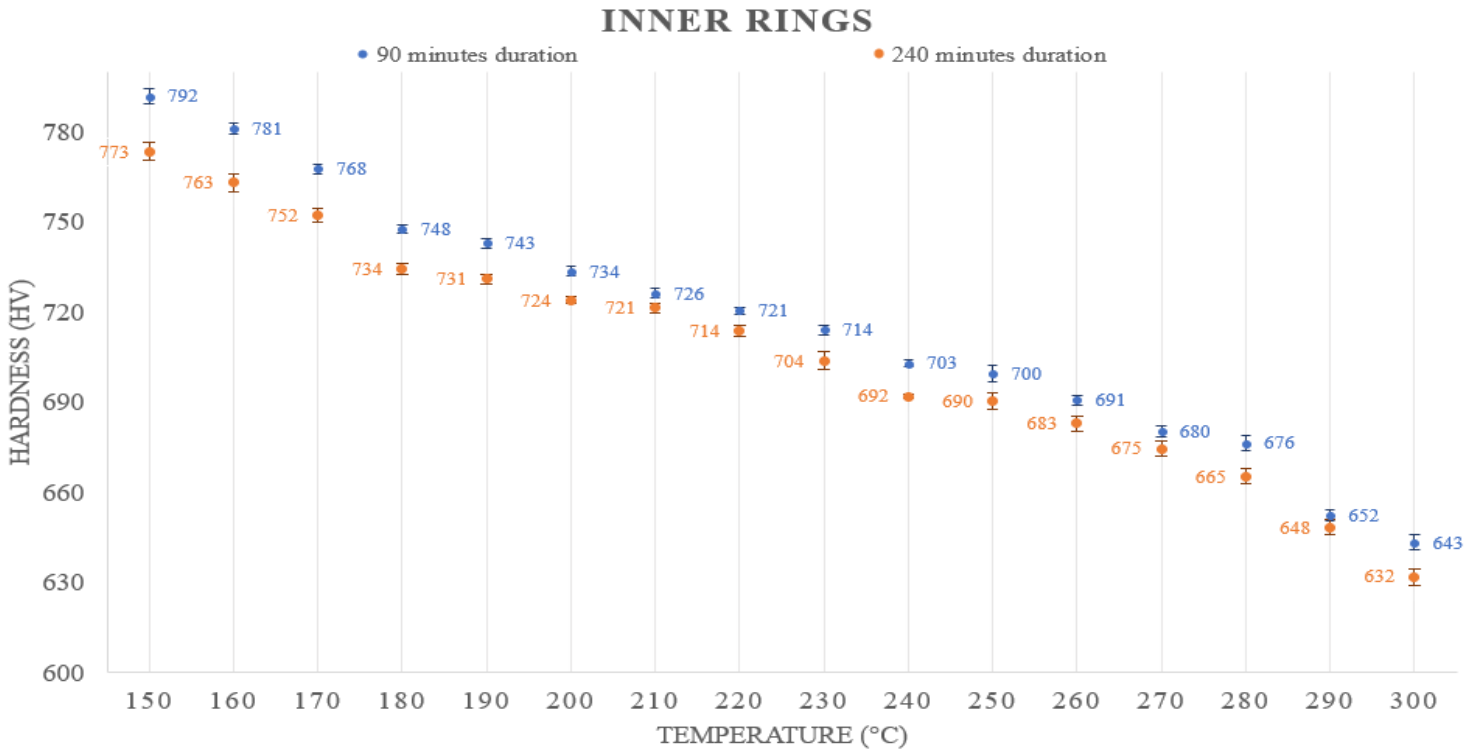

Figure 3.4 Hardness against tempering temperature for inner rings

Figures 3.5-3.8 show hardness change against grain size of carbide for outer and inner rings. It was proved that the hardness of samples obeys Hall–Petch dependency, as the grain size is reduced, the hardness of the samples increases which supports the dislocation pile-up theory. The carbide particles become coarser due to the tempering temperature was increased. This situation caused the decrease in surface area. It has been proved in the Hall-Petch equation, when the surface area of the material is decreased, the hardness of material decreases. The carbide particles want to expand to reach the most stable position. Hence expanded particles cause a decrease in the surface area. The hardness results of both rings were convenient for this phenomenon. In a similar study, the austenitization was performed at 843°C for 30 minutes. Quenched samples were tempered at 150°C. Furthermore, the tempering duration was not shared in the original publication [30]. 100Cr6 steel has brittle properties after the quenched and tempered stage. Tensile test results showed that tensile elongation was nearly % 1-2. Therefore, these results were inconvenient for the comment of tensile properties. The hardness values give more practical information about the tensile strength of rings.

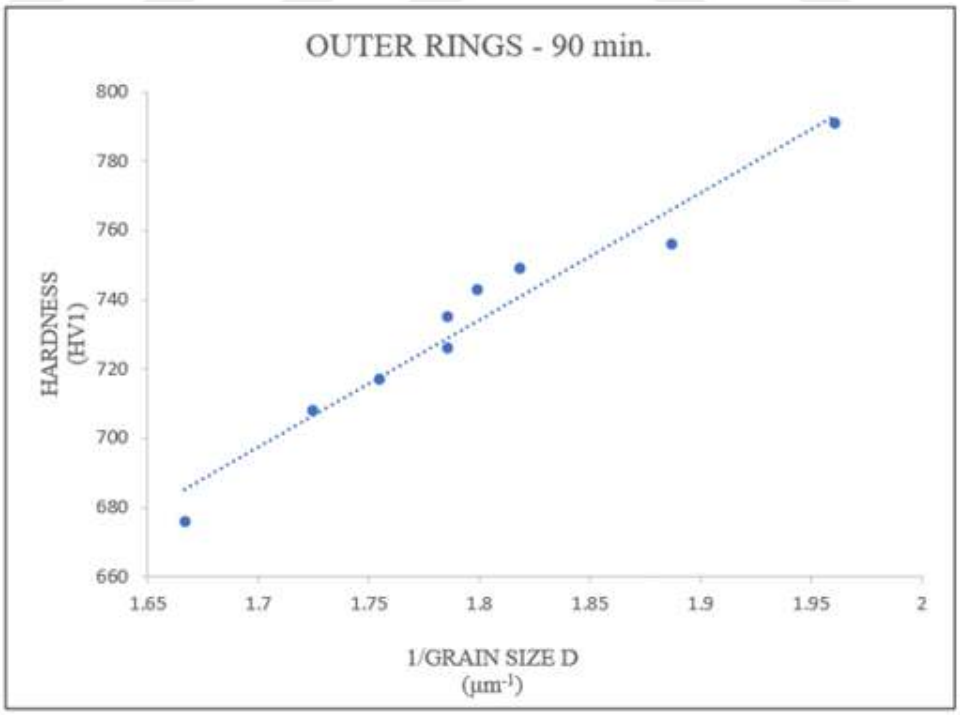

Figure 3.5 Hardness against reciprocal of particle size of carbide

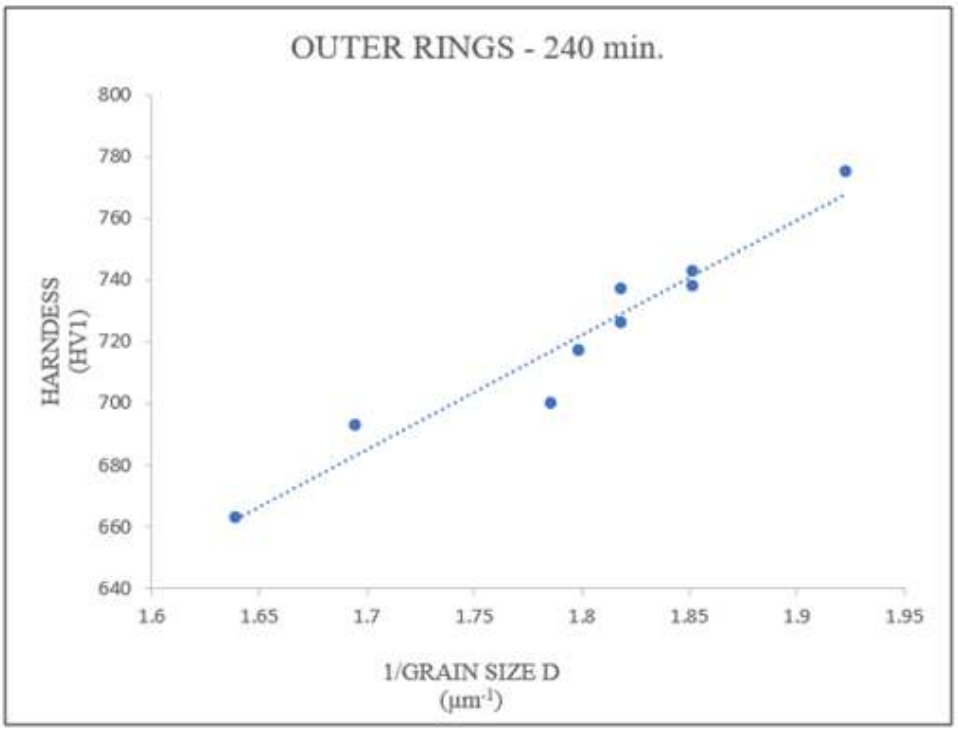

Figure 3.6 Hardness against reciprocal of particle size of carbide

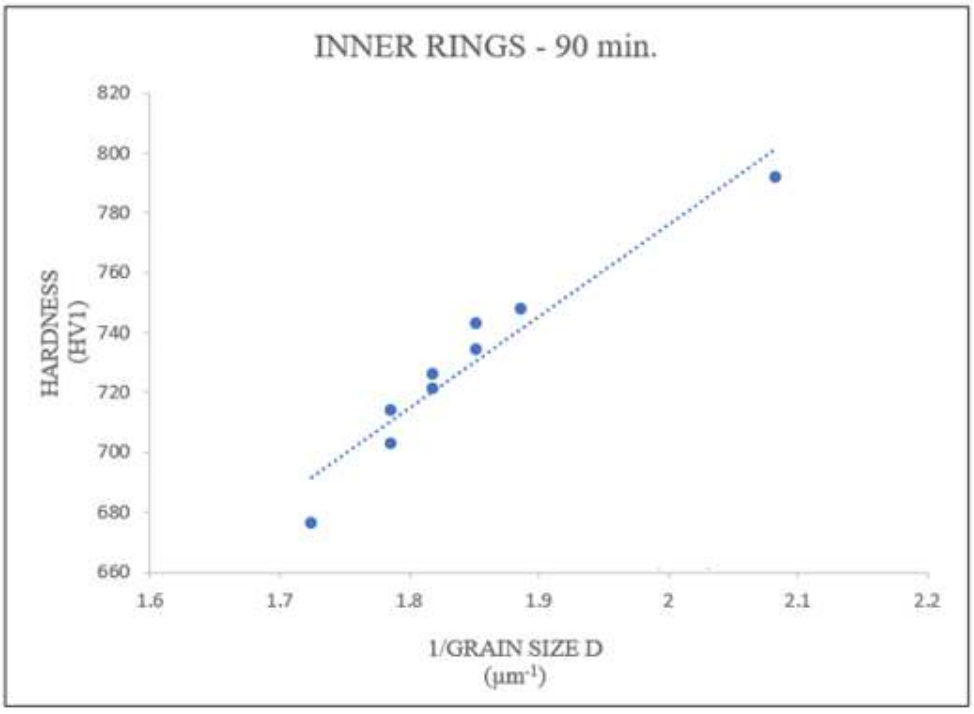

Figure 3.7 Hardness against reciprocal of particle size of carbide

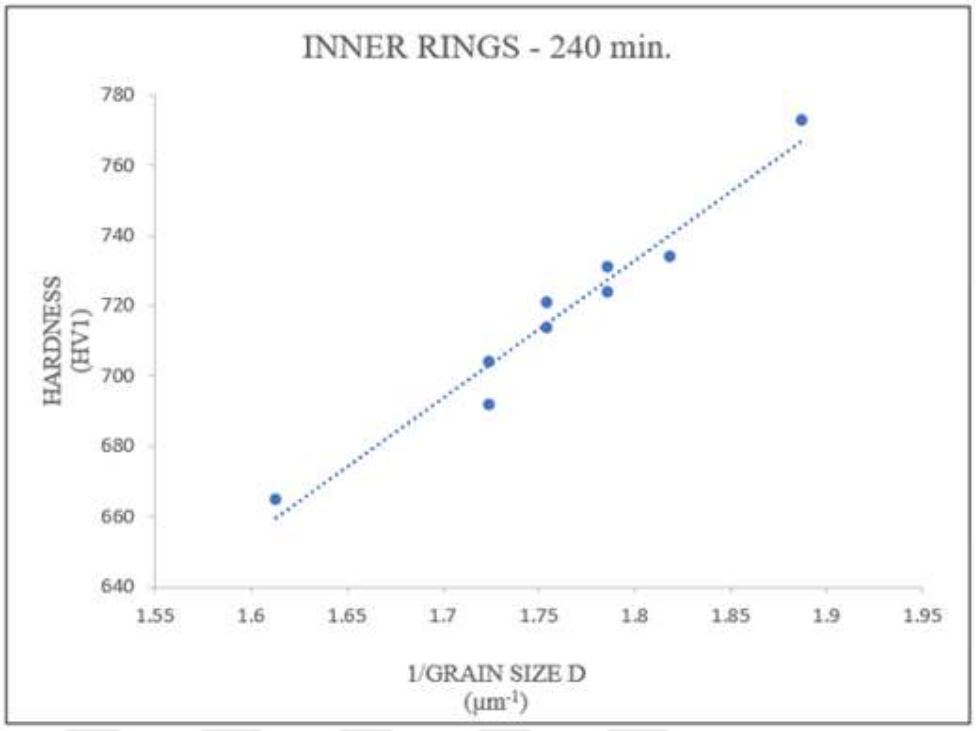

Figure 3.8 Hardness against reciprocal of particle size of carbide

The austenitization temperature is necessary for the formation of hardness up to 850°C. When the austenitization temperature is over 850°C, hardness values do not increase during the quenching process [28] due to the soft retained austenite amount increasing. Therefore, the austenitization temperature was selected by 850°C. It is worth noting that hardness and working temperatures are directly affected by tempering temperatures and durations. Different tempering parameters results showed that mechanical and thermal properties were suddenly changed. Indeed, service life is visibly improved when the hardness exceeds 577 HV1 at ambient temperature [29]. Lower tempering temperatures for rings obtained high hardness values. This type of rings can be used at low operating temperature and high strength applications. Atomic movement restricted at low tempering conditions. Therefore, nonuniform size distribution was observed in carbide particles. Growth was observed on the diameter of rings after the dimensional stabilization test. Higher tempering conditions provided dimensional accuracy. However, hardness values dropped. While they provided high thermal durability, mechanical strength decreased.

CTT diagram in Figure 1.4 has been used to determine the heat treatment parameter for steel. Quenching parameters affect the hardness of samples. These are temperature and duration. However, the diagram does not give any information for tempering conditions. The tempering process is used for stress relaxation of the ring.

Additionally, desired hardness values and other properties are adjusted by them. After the quenching and tempering process, the microstructure of rings consists of tempered martensite, spherical carbides, and retained austenite phases. The fine carbide particles were obtained at lower temperatures. Therefore, the hardness of rings was higher. When the tempering temperature was increased, carbide particles formed coarser, and also hardness dropped as shown in Figure 3.3 and 3.4.

When the tempering temperature is lower than Ms, decomposed austenite amount is less in bearing steel. If the tempering temperature was increased, hardened rings started to be softer, and the stress-strain curve changed. This change can be explained by hardness change.

Hardness reduction was attributed to retained austenite decomposition [31]. When the retained austenite decomposed under loading, the hardness of the sample dropped. Retained austenite cannot be observed under the light optical microscope. This was assumed and accepted according to the XRD results.

The Bauschinger effect was observed in bearing steel due to the austenite phase. The austenite amounts increased dislocation density which provided strain hardening. High tensile strength was caused by dislocations. However, reverse loads led to reduce the number of dislocations. Hence, tensile strength decreased [32]. This situation proved that the hardness is directly affected by the retained austenite amount. For outer rings, dimensional stabilization test results and dimensional change graphs are given in Table 3.1 and Figure 3.9. Distortion is related to the stabilization temperature and retained austenite.

Table 3.1 Average dimensions after stabilization test for outer rings

Sample Denomination	Average Dimensions (mm)
T150-O1	80.04574 (± 0.02346)
T150-O2	80.04512 (± 0.02286)
T180-O1	80.04590 (± 0.02319)
T180-O2	80.04151 (± 0.02096)
T230-O1	79.99802 (± 0.00196)
T230-O2	79.99848 (± 0.00190)
T280-O1	80.00023 (± 0.00064)
T280-O2	80.00056 (± 0.00109)

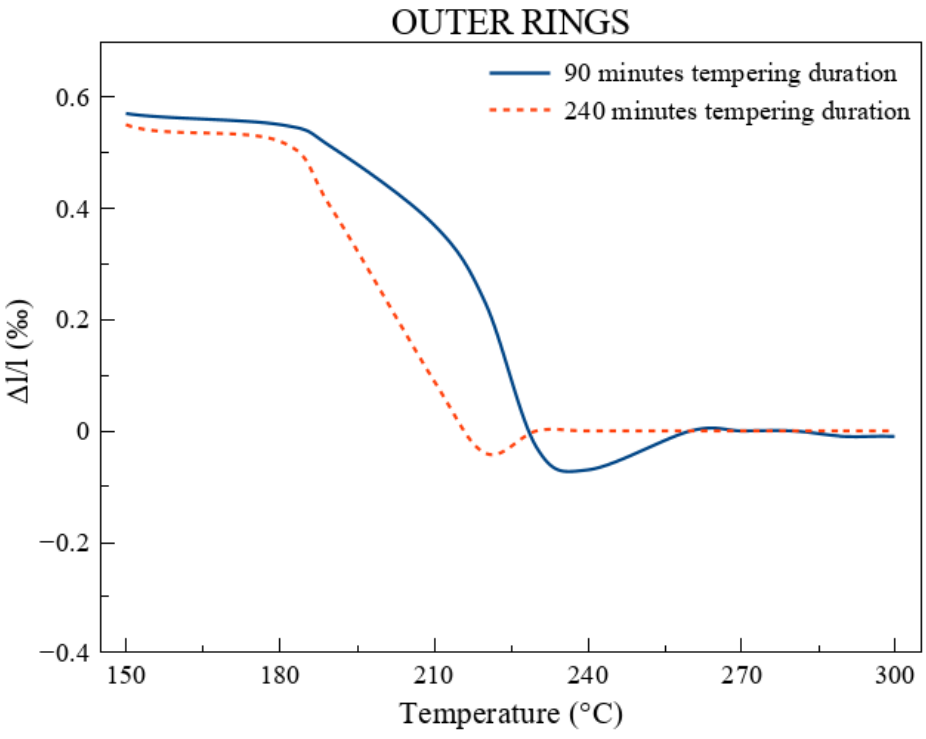

Figure 3.9 Strain percentage against tempering temperature after dimensional stabilization test

For outer diameter measurements, the rings were observed to have enlargement of 45.74 μm and 0.6 ‰ expansion at 150°C for 90 minutes. If bearings are worked in a tight fit region, expansion or shrinkage of rings affects the performance of the bearing in a negative way. Growth was observed to be gradually decreased up to 220°C. It was proved that the decomposition of retained austenite provides dimensional balance. Dimensional change was not observed at 220°C due to the retained austenite content which was less than 1 vol.%. When rings include approximately 1 vol % [41] of retained austenite content, dimensional balance is ensured. Shrinkage was observed as -1.98 μm at 230°C. It was proved that fully decomposed retained austenite causes approximately 2 vol % rings contractions. Dimensional stability was provided again at 260°C.

Table 3.2 Average dimensions after stabilization test for inner rings

Sample Denomination	Average Dimension (mm)
T150-I1	40.03966 (± 0.02004)
T150-I2	40.04138 (± 0.02113)
T180-I1	40.02778 (± 0.01399)
T180-I2	40.02461 (± 0.01244)
T230-I1	40.00329 (± 0.00628)
T230-I2	39.99726 (± 0.00173)
T280-I1	39.99881 (± 0.00103)
T280-I2	39.99936 (± 0.00137)

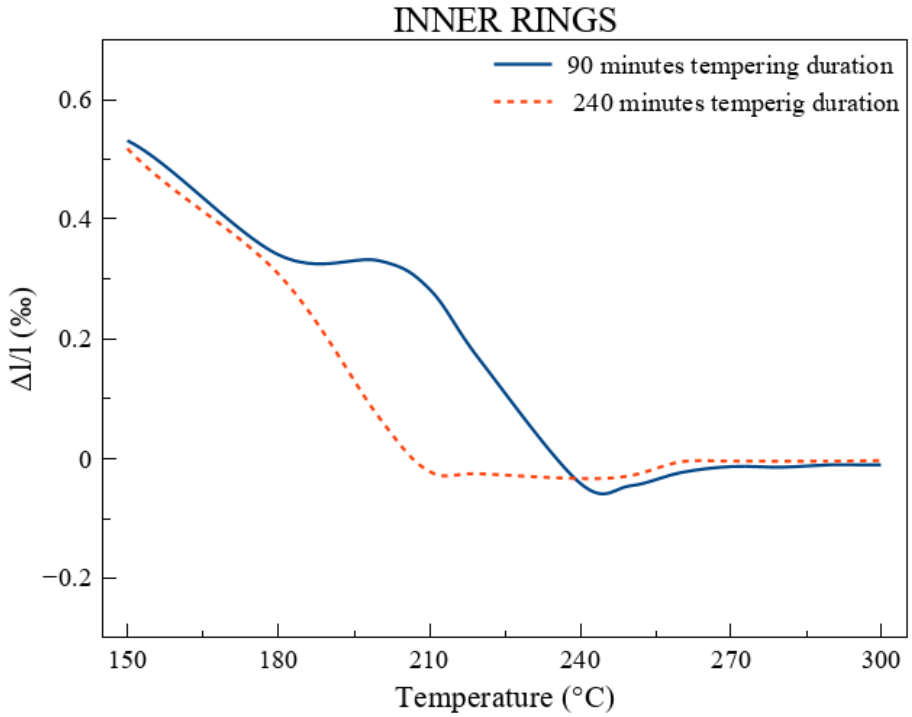

Figure 3.10 Strain percentage against tempering temperature after dimensional stabilization test

Dimensional change of inner rings (Figure 3.10) was observed to expand 39.66 µm and -0.52 ‰ of size distortion at 150°C for 90 minutes. Due to higher tempering temperature, austenite started to decompose into martensite, and dimensional distortion could be easily controlled before the stabilization test. Owing to the complete decomposition of the retained austenite, dimensional change was not observed between 230°C and 290°C.

Due to the diameter of inner rings being half of the outer diameter (Figure 2.1), the range of atomic motion was restricted during the through hardening treatment. With increasing temperature up to 230°C and 220°C for inner and outer rings respectively, enlargement was observed to decrease for both rings due to the decomposition of the retained austenite. Dimensional change was not observed after 240°C for inner rings and 260°C for outer rings. Expansion of inner rings was less than outer rings at lower temperatures.

Dimensional stabilization was observed on inner rings before outer rings. This occurred because the decomposition of retained austenite was completed for inner rings at a lower temperature than outer rings.

Fatigue performance is directly related to dimensional balance. Retained austenite affects the dimensional stability of bearing negatively. According to the simulation studies, retained austenite causes localized stress and volume expansion on rings [42, 43]. Decomposition of retained austenite varies by diameter, thickness, and shape of sample in tempering conditions. These parameters cause an increase in complexity. Therefore, an acceptable assumption is difficult but necessary in tempering conditions. The elastic structure of bearings is improved by less amount of retained austenite content. Similar studies have been observed to include phase transformation and annealing reactions about dimensional distortion in the bearing steels.

Dimensional stability is a crucial parameter against elastic expansion at high rotation applications in aerospace and automotive industries. Unfortunately, it was not mentioned in literature studies. The phase can be reduced to a minimum by using a suitable tempering heat treatment. Decomposition of retained austenite leads to distortion of bearings throughout service life. Dimensional change parameters have been defined by Mayr [33]. For instance, the fitting of bearing on shafts is related to the dimensional tolerances on bearings. If the bearing has a distortion, the bearing cannot be mounted to the shaft.

If through-hardened rings are tempered between 50 and 150 °C, e-carbide arises as a first precipitated phase. It leads to a shrinkage of nearly $10^{-4,}$ which can be accepted in a negligible strain range [34, 35]. If the tempering conditions are appropriate for the precipitation of cementite, enlargement can be observed on rings diameter. Enlargement led by decomposition of retained austenite dominates the shrinkage caused by the e-carbide phase. The acquired strain is nearly 10^{-3} percent of decomposed retained austenite in bearing rings. Similar studies show that dimensional change is related to phase transformation and tempering conditions [36-38].

The decomposition of retained austenite into martensite leads to dimensional instability. This occurs because the intensity of parent phase is greater than the product

phase. Growth is approximately 4um per 100 mm [39]. Such changes have been measured for bearing steels, and although the heat treatment conditions were not fully reported, the strain increases as the transformation is suppressed to lower temperatures [40]. When the transformation occurred at lower temperatures, the difference in density was increased because the thermal expansion coefficient of austenite is much higher than ferrite.

3.4 Effect of Tempering Duration on Mechanical and Physical Properties

As the tempering duration was increased, the hardness values were decreased, as given in Figure 3.3 and Figure 3.4. The hardness of 90 minutes tempered rings was higher than 240 minutes tempered rings. This situation showed that desired hardness value could be achieved by tempering rings at lower temperatures for a longer time. The tensile test is inconvenient for 100Cr6 steel because the strain is lower than 2% [38]. Therefore, hardness values can be used for getting information about tensile strength. According to the Larson miller parameter, the strength of the rings against the applied force is proportional to the tempering temperature and duration. For the outer rings, the hardness values were 790 HV1 and 775 HV1, at 150°C for 90 and 240 minutes tempering, respectively. The hardness values decreased by increasing the temperature and duration. The hardness value dropped to 756 HV1 for 90 minutes and 743 HV1 for 240 minutes at 180°C tempering. At 230°C, the hardness value was reduced from 717 HV1 to 700 HV1 by increasing the tempering duration. Finally, hardness values were same as 650 HV1 for 90 and 240 minutes tempering duration at 300°C.

For outer rings, the 240 minutes tempering duration comprised uniform hardness than 90 minutes tempering around the ring. Longer tempering duration provided more e-carbide precipitation at 150 and 160 °C, faster retained austenite decomposition at 170 and 230 °C, and coarser carbon particles on rings at 230 and 300 °C tempering.

The hardness value was respectively 792 HV1 and 773 HV1, at 150°C for 90 and 240 minutes tempering for the inner rings. As a result, the temperature and duration, hardness decreased. The hardness value decreased to 748 HV1 for 90 minutes and 734 HV1 for 240 minutes at 180°C. The hardness values reduced to 714 HV1 for 90

minutes and 704 HV1 for 240 minutes at 230°C. At 300°C tempering conditions, similar results were obtained for 90 and 240 minutes tempering durations.

For inner rings, the 240 minutes tempering duration comprised uniform hardness than 90 minutes tempering around the ring. Longer tempering duration provided more e-carbide precipitation at 150 and 170 °C, faster retained austenite decomposition at 180 and 230 °C, and coarser carbon particles on rings at 230 and 300 °C tempering.

The diameter of the inner rings had half the diameter of the outer rings. The tempering temperature and duration were increased, the tempering parameter value increased, and the resistance of the rings against external stress was decreased. Thus, the hardness value dropped.

It has been observed that the effect of the tempering duration for inner rings was observed more distinctive than outer rings.

3.5 Effect of Tempering Temperature on Microstructure

Microstructure evaluation of the rings is given in Figure 3.11 and Figure 3.12. Images from optical microscopy, image analysis and SEM were summarized for the samples tempered at 150, 180, 230 and 280ºC.

In Figures 3.11 and 3.12, undissolved carbide particles and martensite phase seem on SEM images. Undissolved carbides amount and size were smallest at lower tempering conditions same the stage 1 tempering conditions. When the tempering temperature increased up to 180°C, undissolved carbides were distinctly expanded due to reducing the retained austenite. In stage 2 tempering condition the martensite phase starts to diffuse into the cementite structure. The size of carbide particles became larger. Whereas fraction area of carbide particles increased, surface area decreased. Hence hardness of samples decreased.

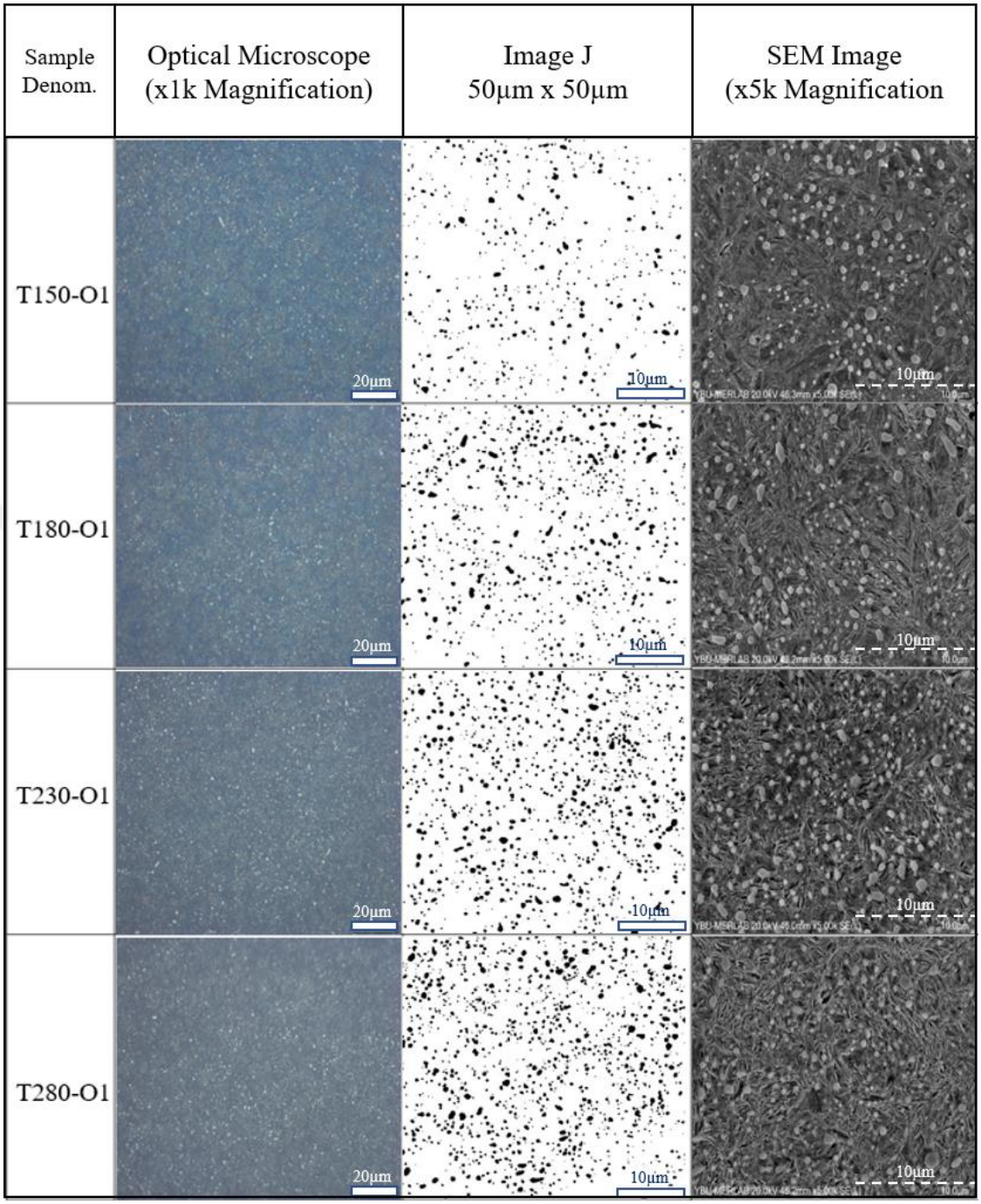

Figure 3.11 Images of outer rings tempered for 90 minutes

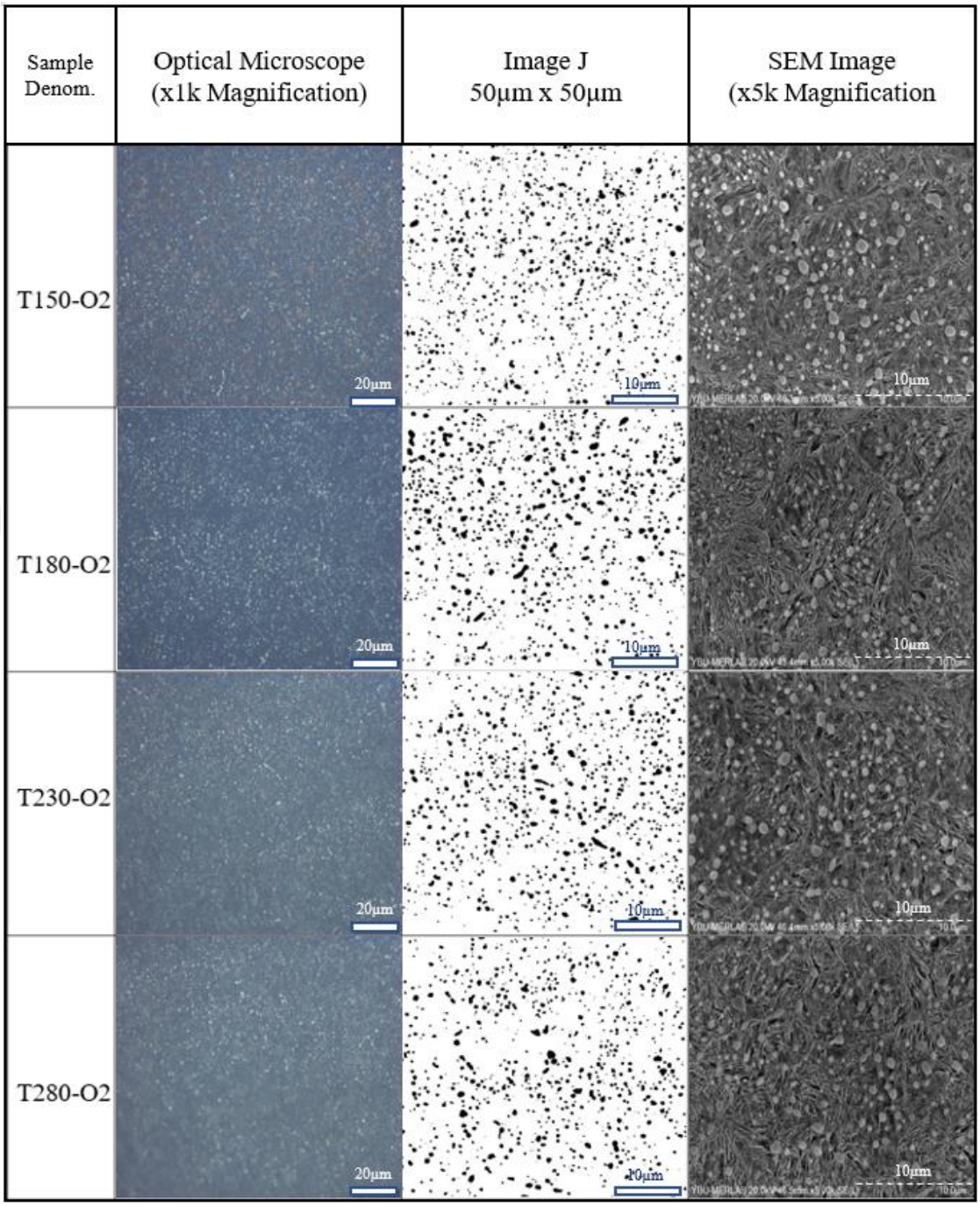

Figure 3.12 Images of outer rings tempered for 240 minutes

Carbide particles were restricted by retained austenite at lower temperatures and duration. The temperature was insufficient for being dominant carbide phases. Retained austenite started to decompose into the martensite phase at 180°C. At higher temperatures, atomic motions of carbide particles were faster, and decomposition of

the retained austenite accelerated. When the tempering temperature reached Ms temperature, the amount of retained austenite was zero.

Fraction area of carbide particles restricted by e-carbide, retained austenite and lower tempering duration at stage 1 tempering condition. It blocked the expansion of particles due to the high stress and retained amount. Ninety minutes tempering duration was not convenient for dissolution of e-carbide and retained austenite. Hence fraction area is lower at stage 1 tempering condition for 90 minutes tempering duration.

The fraction area of particles was similar at stage 2 and stage 3 tempering conditions due to the phase transformation and retained austenite decomposition. Longer tempering duration provided the high fraction area at lower tempering temperatures. Heat comprised all around the samples for a longer time. Hence carbide particles moved easier than low duration.

Table 3.3 Size and fraction area of carbide particles in outer rings

Sample Denomination	Carbide Size (μm) Std. Dev.	Fraction Area (%)
T150-O1	0.51 ± 0.20	7
T150-O2	0.52 ± 0.19	15
T180-O1	0.53 ± 0.21	12
T180-O2	0.55 ± 0.24	16
T230-O1	0.57 ± 0.20	16
T230-O2	0.56 ± 0.21	16
T280-O1	0.60 ± 0.22	18
T280-O2	0.61 ± 0.23	16

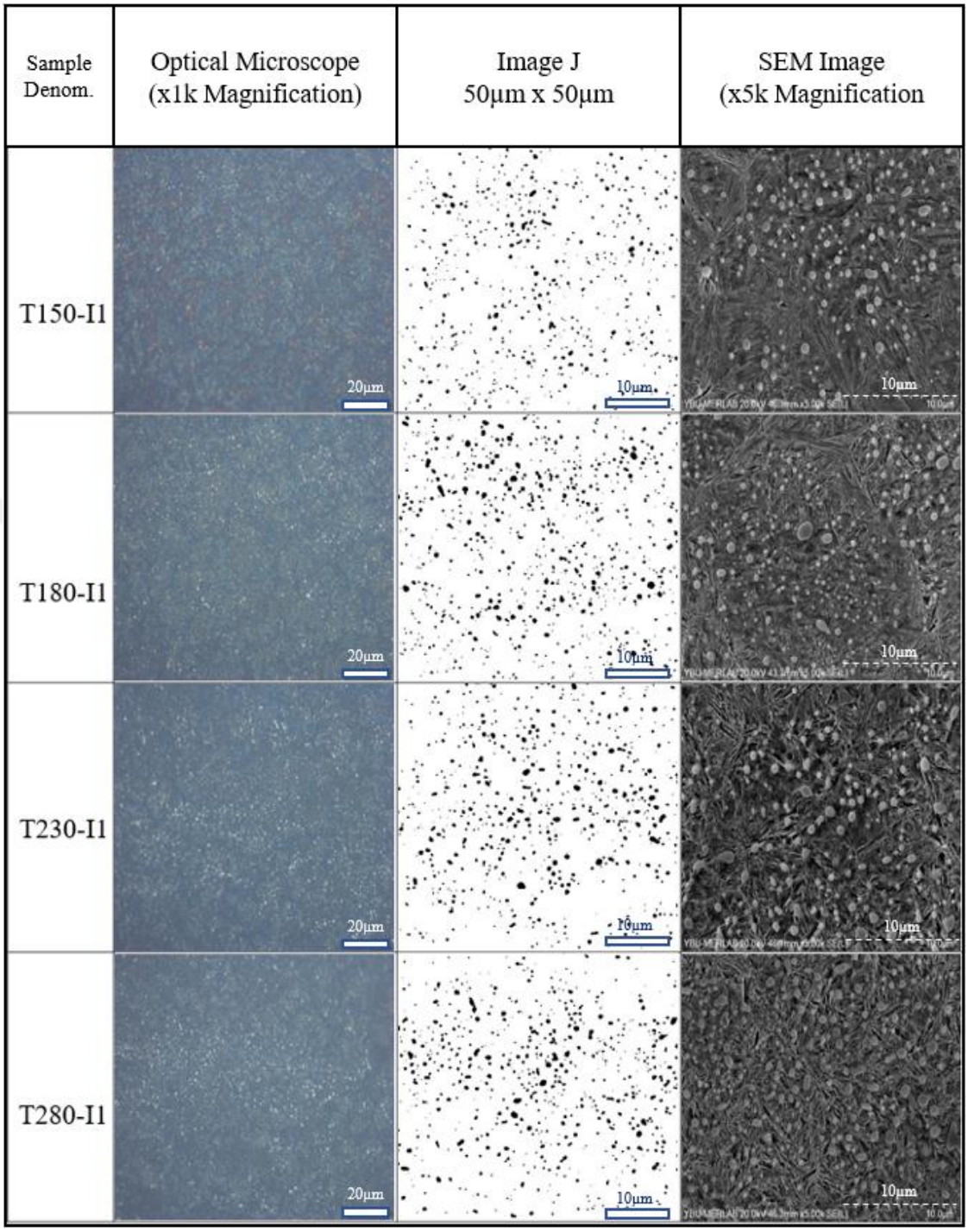

Figure 3.13 Images of inner rings tempered for 90 minutes

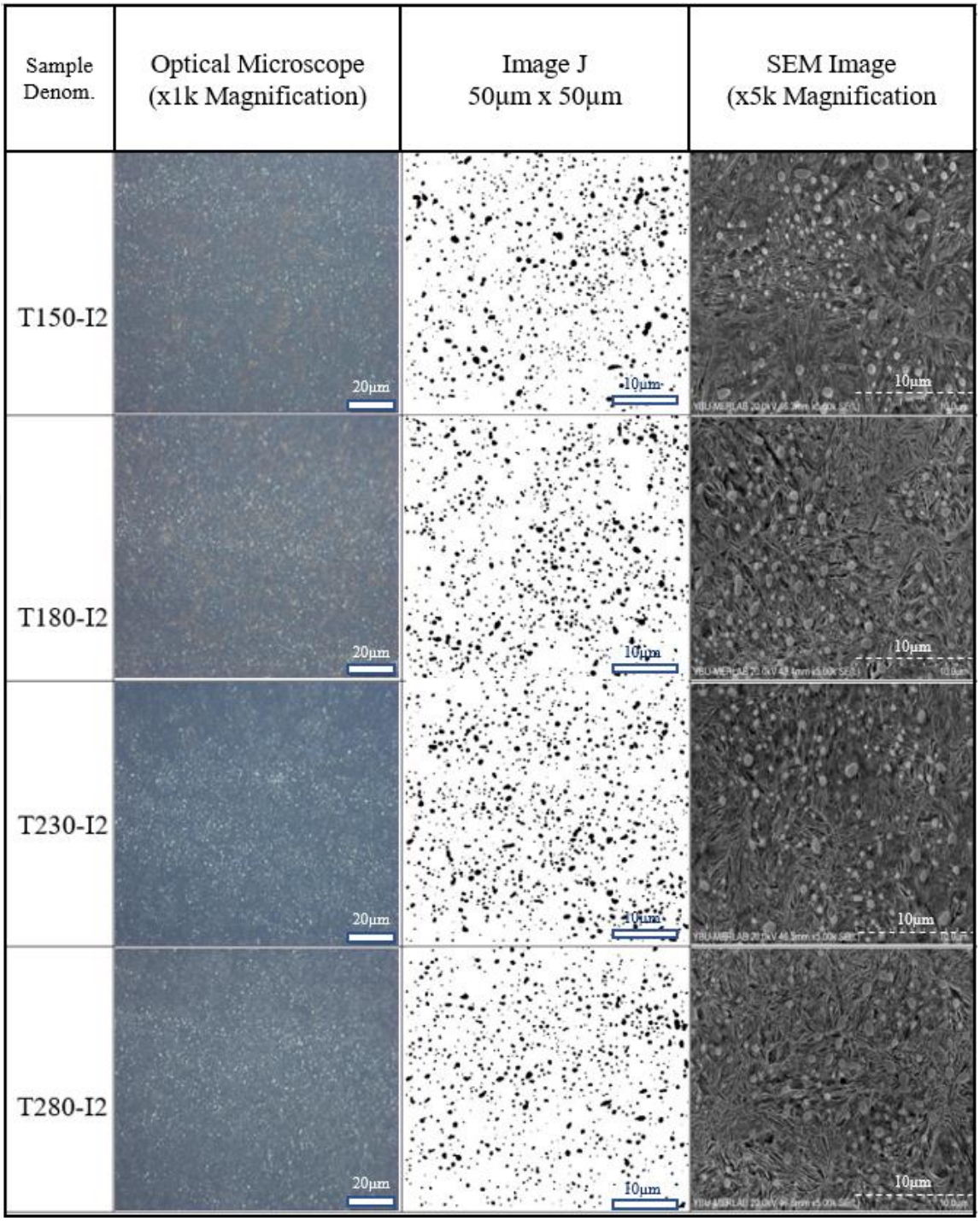

Figure 3.14 Images of inner rings tempered for 240 minutes

In Table 3.4 for inner rings with 90 minutes duration, the particle size of carbides and fraction area were respectively 0.48 μm and 9% at 150°C tempering condition, 0.53 μm and 11% at 180°C, 0.56 μm and 19% at 230°C and finally 0.58 μm and 17% at 280°C.

In Figures 3.13 and 3.14, undissolved carbide particles and martensite phase are examined in SEM images. Undissolved carbides amount and size were smallest at lower tempering conditions similar to outer rings. When the tempering temperature increased up to 230°C, undissolved carbides were distinctly expanded due to reducing the retained austenite. In stage 2 tempering condition the martensite phase starts to diffuse into the cementite structure. The size of carbide particles became larger. Whereas fraction area of carbide particles increased, surface area decreased. Hence hardness of samples decreased.

The fraction area of particles was similar at stage 2 and stage 3 due to the phase transformation and retained austenite decomposition. A longer tempering duration was effective at 180°C. At upper temperatures, while particle size increased, fraction area was not distinctly changed.

Table 3.4 Size and fraction area of carbide particles in inner rings

	Carbide Size (μm) Std. Dev.	Fraction Area (%)
T150-I1	0.48 (±0.16)	9
T150-I2	0.53 (±0.21)	11
T180-I1	0.53 (±0.20)	11
T180-I2	0.55 (±0.28)	17
T230-I1	0.56 (0.23)	19
T230-I2	0.58 (±0.23)	19
T280-I1	0.58 (±0.19)	17
T280-I2	0.60 (±0.25)	16

The diameter of inner rings is two times smaller than outer rings. So that tempering temperature and diameter differences of samples were affected by the rings. According to experimental results, the amount of the retained austenite was decreased when the particle size of carbides and fraction area of carbides were increased.

The carbide sizes of the inner rings and outer rings were similar for the same tempering condition. However, the fraction area of inner rings restricted according to outer rings for 90 minutes tempering. Due to the diameter difference, inner rings did not have enough area for carbide particles. According to the tempering condition results, 90 minutes tempering duration was not adequate for inner rings, while the fraction area of outer rings was observed to increase by 90 minutes tempering duration.

Steels with a carbon content of 0.8-1.1 wt.% were preliminarily designed for manufacturing tools and gradually dominated the bearing market [44, 45]. The intention of spheroidisation is to obtain a softer material by coarsening the microstructure. The carbide particles have a size in the range of 0.5-3 μm after the spheroidisation annealing condition [46]. Using spheroidisation annealing, the size of the carbides can be controlled when followed by the usual quenching and tempering condition. It has been demonstrated that there is a benefit from a fatigue perspective on having a precision dispersion in the spheroidisation annealing. In this way, undissolved carbides can be small in size as well [47,48]. Repeating the annealing with a second tempering treatment at a lower temperature is necessary for the separation of the networks [49].

Quenching from the austenitization forms a microstructure involving martensite, about 6 vol.% of retained austenite and 3-4 vol.% of cementite particles which failed to dissolve during austenitization [50,51]. The particle size of samples is about 0.4-0.6 μm which are uniformly distributed. The austenite phase transformed to martensite by quenching process. The martensite phase was hard and brittle. As a result, tempering conditions provided relaxation and homogenization on the rings.

The martensite is based on carbon in solid solution and fine transition carbides of iron, predominantly e-carbide for its strength [52].

The rings were tempered between at 150°C to 300°C, a tempering process that may lead to the separation of retained austenite and the sedimentation of varied transition carbides of iron (ferrite) from the supersaturated martensite.

3.6 Effect of Tempering Duration on Microstructure

Longer tempering time both increased particle size and fraction area of outer rings even in lower temperatures. In Table 3.3, the particle size of carbides of T150-O1 and T150-O2 were closely 0.51 μm and 0.52 μm while the fraction area increased from 7% to 15%. The differences between the particle size of carbide were 0.02 μm, however the percentage fraction area of samples was observed to expand from 12% to 16 %. The carbide particles and fraction area increased to 0.57 μm and 16 % respectively at 230 °C due to complete decomposition of the retained austenite into martensite phase and supersaturation of the martensitic microstructure. However, the longer tempering duration at 230°C did not cause distinguishable changes in the microstructure and fraction area. This situation can be explained by the fact that carbide particles have reached the fraction area where they have maximum dominance. When rings were tempered at 230°C and above temperatures, dimensional stabilization was provided. It was proved that retained austenite caused dimensional distortion on rings.

Therefore, it can be said that 90 minutes tempering duration is not sufficient for inner rings. The carbide grain sizes and fraction area of the samples named T150-I1 and T150-I2 were 0.48 μm to 0.53 μm and 9% to 11% respectively. While the carbide particle sizes were 0.53 μm and 0.55 μm T180-I1 and T180-I2, the fraction area is 11% and 17% respectively. Compared to lower temperature conditions, the sizes of carbide particles increased at higher tempering temperatures. The fraction area changes are related to tempering duration. According to results, the carbide particle sizes slowly expanded from 0.48 μm to 0.60 μm, when the temperature increased from 150°C to 300°C. Additionally, the fraction area of the carbide increased up to 9% to 19%.

Due to the small diameter of the ring, the motion range of atoms is limited. When the retained austenite effect is added, the atomic motion is further restricted and the growth

of carbide grains prevented. Inner rings had enough area for carbide particles growth in 240 minutes tempering conditions. Outer rings had less fraction area than inner rings in 240 minutes duration.

In Figure 1.7, the samples completed the stress relaxation in 240 minutes at lower temperatures. It showed that microstructural homogenization occurred at this condition because of the decomposed retained austenite. The retained austenite can be continuously decomposed at each temperature, but the decomposition rate of samples was affected by durations. The size, diameter and thickness of the samples are influential factors on conversion rate. Experimental parameters can change the decomposition rate of the retained austenite amount. Therefore, it is not appropriate to generalize the decomposition rate as if there was only one fact. It has been observed that tempering durations have different effects on outer rings with a diameter of 80 mm and inner rings of 40 mm. Time-saving is a crucial point for the yield of manufacturing. Duration is a considerable process stage of tempering. Stress relaxation percentage was not changed in longer tempering duration than 240 minutes at close temperatures. According to the test results, 240 minutes of tempering duration can be determined as the ideal time for the dimensional stabilization and microstructural homogenization of 40-80 mm diameter rings.

CHAPTER 4

CONCLUSION

In this thesis, various temperature and duration values were studied during the heat treatment of 100Cr6 bearing steel and their effects on retained austenite, physical-mechanical properties and microstructure were investigated.

1. A gradual (three-step) decrease was observed in the amount of retained austenite against increasing tempering temperature and duration. For outer rings a slight decline was observed until 180°C for both durations while an abrupt drop was obtained up to 210°C. For 240 minutes, retained austenite was completely decomposed into martensite at 220°C while consumption of the phase completed at 230°C for 90 minutes. Increasing tempering duration provided a 10°C reduction. For inner rings slow decrease was observed until 200°C for 90 minutes duration while rapid degradation was obtained until 180°C for 240 minutes. Retained austenite dropped suddenly to 200-240°C for 90 minutes. It was completely decomposed into martensite at 230°C for 90 minutes and at 210°C for 240 minutes. Increasing tempering duration assured a 20° decline.

2. With increase of the tempering temperature and duration, the hardness decreased and ranged 775-658 HV1 for 240 minutes and 790-658 HV1 for 90 minutes. Even the hardness values were higher for 90 min at the lower temperatures, the difference was disappeared at higher temperature. The amount of retained austenite has directly affected the change in hardness value at lower temperatures. When the rate of retained austenite degradation increased, stress relaxation raised. Hence hardness values decreased. Similar situation was observed on inner rings. The hardness value decreased and reached 792-643 HV1 for 90 minutes and 773-632 HV1 for 240 minutes.

3. Rise in both duration and temperature provided dimensional stability for inner and outer rings. Dimensional distortion reduced to 0.56 μm from 45.74 μm for outer rings as a result of retained austenite consumption. For inner rings negative distortion values

at higher temperatures decreased from 39.66 μm to -0.64 μm. Dimensional stabilized bearings which prevents high amount distortion, ensure long service life. Dimensional expansion amount at lower temperatures was high for bearing manufacturing due to the retained austenite. Technical drawing of rings must be designed according to dimensional distortion. The tempering duration parameter of 6208 type bearing was changed from 90 minutes to 240 minutes according to the dimensional results of this thesis. Also, tempering temperatures were upgraded to temperatures at which minimum dimensional change was observed. These temperatures were selected according to heat stabilization classes.

4. The microstructure of tempered samples mainly consisted of the tempered martensite and spherical carbides. The amount, size and fraction area of carbide particles raised at higher tempering temperature and duration, especially at Stage 2 and 3. The particle size growth occurred to 0.51μm from 0.61 μm for outer rings. Similar values observed for inner rings. With the expansion of carbide particle sizes, the surface area declined for rings. This situation caused the hardness reduction. The enlargement of fraction area was 8-18% for outer rings and 9-19% for inner rings. The particle size distribution was homogeneously observed. It provided dimensional stability for both rings.

4.1 Suggestions for Future Work

- Dimensional stabilization testing for thinner and thicker dimensions of rings
- Increasing the tempering temperature
- Using variable dimensional test conditions according to the tempering temperatures
- Fatigue life testing for stabilized bearings
- Measuring internal stress before and after stabilization test
- Friction testing of rings

REFERENCES

[1] R.E. Reed-Hill, “Physical Metallurgy Principles”, D. Van Nostrand Co., New York, 1973, pp. 701-747.

[2] Agostino Ramelli, “Plate 192: Ballista. In Le Diverse Et Artificiose Machine Del Capitano Agostino Ramelli”, Paris, France, https://www.digital.sciencehistory.org/works/js956g141, [Visited Date:10 November 2020].

[3] Intech Bearing Inc., “Double-Row Angular Contact Ball Bearings”, https//www.intechbearing.com/collections/5200-series-angular-contact-ball-bearings, [Visited Date : 11 May 2020]

[4] W. D. Callister and D. G. Rethwisch, “Material Science and Engineering: An Introduction”, New York: Jhon Wiley& Sons, 2007.

[5] Stribeck, R., “Kugellager für beliebige Belastungen (Ball Bearings for any Stress)”, Zeitschrift des Vereins Deutscher Ingenieure 45, Germany, 1991.

[6] G. F. Vander Voort, “Atlas of Time-Temperature Diagrams for Irons and Steels”, ASM International, p.96, 1991.

[7] Ovako Steel Navigator, “Material Data Sheet”, Sweden, https://www.steelnavigator.ovako.com/steel-grades/100cr6/, [Visited Date: 09 June 2021].

[8] Chae, Jae-Yong, “Application of Lower Bainite Microstructure for Bearing Steels and Acceleration of Transformation Kinetics”, Thesis for Doctor of Philosophy, Computational Metallurgy Graduate Institute of Ferrous Technology Pohang University of Science and Technology, 2012.

[9] Guillot M, Dudragne G., “Optimisation of the thermal treatment of a roller bearing steel 100Cr6”, Memoires Etudes Scientifiques Rev. Metallurgy, 79, p. 493, 1982

[10] Tsubota K, Sato T, Kato Y, Hiraoka K, Hayashi R., Bearing steels in the 21st century, Pennsylvania (USA): American Society for Testing of Materials, p. 202–15, 1998.

[11] C.S. Roberts, B.L. Auerbach, and M. Cohen, The Mechanism and Kinetics of the First Stage of Tempering, Trans. ASM, Vol 45, p 576-604, 1953.

[12] B.S. Lement, B.L. Auerbach, and M. Cohen, Microstructural Changes on Tempering Iron Carbon Alloys, Trans. ASM, Vol 46, p 851-881, 1954.

[13] F.E. Werner, B.L. Auerbach, and M. Cohen, The Tempering of Iron Carbon Martensitic Crystals, Trans. ASM, Vol 49, p 823-841, 1957.

[14] G.R. Speich, Tempered Ferrous Martensitic Structures, in Metals Handbook (8^{th} ed.), American Society for Metals, Vol.8, p 202-204, 1973.

[15] Pearson, P. K., Size Change of Through Hardened Bearing Steels at Application Temperatures, SAE Trans. A, Vol. 106(2), p 170–175, 1997.

[16] Duval, P., Murry, G., and Constant, A., Stabilite´ Dimensionnelle dans le Temps. Contributiona` l'Etude des Facteurs Me´tallurgiques Affectant la Stabilite´ Dimensionnelle des Aciers, Me´c. Electr., pp. 28–37, 1968.

[17] Gerberich WW, Thomas G, Parker ER, Zackay VF. Metastable austenites: decomposition and strength, In: Second international conference on strength of metals and alloys,1970, Ohio (USA): ASM International, p. 894–9, 1970.

[18] Hokkirigawa K, Kato K, Li ZZ. The effect of hardness on the transition of the abrasive wear mechanism of steels, 123, p 241–51, 1988.

[19] R.E. Reed-Hill, Physical Metallurgy Principles, D. Van Nostrand Co., New York, p 701-747, 1973.

[20] G.V. Kurdjumov, L.M. Utevskij, Metallovedenie i termičeskaja obrabotka stalji, Metallurgija, Moskva, p. 174, 1983

[21] Zoran Janjusevic, Zvonko Gulisija, Marija Mihailovic, Aleksandra Pataric, “The investigation of applicability of the hollomon-jaffe equation on tempering the HSLA steel”, Serbia, p. 131-136, 2009.

[22] Brown R.L., Cohen M., “Stress relaxation of hardened steel”, Met. Prog. 83, p 66–71, 2009.

[23] NSK Rolementos, “Catalog E728g”, https://www.nsk.com.br/rolamentos-144.htm, Brasil, [Visited Date: 20 September 2021].

[24] Naik, S.N., Walley, S.M., “The Hall-Petch and inverse Hall-Petch relations and the hardness of nanocrystalline metals”, J Mater Sci, 55, p 2261-2681, 2020.

[25] Armstrong R.W., ”60 years of Hall–Petch: past to present nanoscale connections”, Mater. Trans., 55, p 2–12, 2014

[26] Hewitt W., “The spheroidise annealing of high carbon steel and its effect on subsequent heat treatment”, Heat Treated Met.,3, p 56–62, 1982.

[27] Matas S., Hehemann R.F., “Retained austenite and the tempering of martensite”, Mat. Nature, 187, p 685–6, 1960.

[28] Huh M.Y., Bae K.K., Kim S.J., “A study on the mechanical properties and substructures of 1.0%C–1.4%Cr bearing steel”, J Korean Inst. Met., 20, p 987-94, 1982.

[29] Baughman R.A., “Effect of hardness, surface finish, and grain size on rolling-contact fatigue life of M50 bearing steel”, J Basic Eng., 82, p 287–94, 1960.

[30] Shi J., Liu C.R., “On predicting chip morphology and phase transformation in hard machining”, Int. Advance Manufacturing Technology, 27, p 645–54, 2005.

[31] Beswick J.M., “Fracture and fatigue crack propagation properties of hardened 52100 steel”, Metall. Mater. Trans., 20, p 1961–73, 1989.

[32] Simsir C, Dalgiç M, Lübben T, Irretier A, Wolff M, Zoch HW., "The Bauschinger effect in the supercooled austenite of SAE 52100 steel", Acta. Mater. 58, p 4478–91, 2010.

[33] Mayr P., "Dimensional alteration of parts due to heat treatment", Residual stress in science and technology (vol. 1), DGM-Informationsgesellschaft-Verlag, Oberursel (Germany), 1987.

[34] Averbach B.L., Cohen M., Fletcher S.G., "The dimensional stability of steel: Part III. Decomposition of martensite and austenite at room temperature", Trans. ASM, 40, p 728–43, 1948.

[35] Hengerer F, Nierlich W, Volkmuth J, Nützel H., "Dimensional stability of high carbon bearing steels", Ball Bearings J, 231, p 26–31, 1988.

[36] Palermo H.F., Flinn R.A., "Dilation due to austenite transformation as a function of temperature and composition", Trans Am Foundrymen's Society, 83, p 503–18,1975.

[37] Malecki P., Langer E.W. "Dissolution of cementite with alloying elements in austenite", Scand J. Metall., 19, p 182–6, 1990.

[38] Ovako Steel Navigator, "Material Data Sheet", Sweden, https://www.steelnavigator.ovako.com/steel-grades/100cr6/, [Visited Date: 09 June 2021].

[39] Neu RW, Sehitoglu H., "Transformation of retained austenite in carburized 4320 steel", Metall. Mater. Trans., 22, p 1491–500, 1991.

[40] Daguier P., Roesch O., Trojahn W., "New development in through hardened bearing steel grades for use in contaminated lubricants", J. ASTM Int., 3, p 140-45, 2007.

[41] Mikus E.B., Hughel T.J., Gerty J.M., Knusden A.C., "The dimensional stability of a precision ball bearing material", Trans. ASM, 52, p 307–20, 1960.

[42] Alley E.S, Neu RW., “Microstructure-sensitive modeling of rolling contact fatigue”. Int J Fatigue, 32, p 841–50, 1960.

[43] Alley E.S., Swamiphakdi K., Anderson P.I., Neu R.W., “Modelling the influence of microstructure in rolling contact fatigue”, J ASTM Int., 7, p 1026-29, 2010.

[44] Bamberger E.N., “Materials for rolling element bearings” Bearing design – historical aspects, present technology and future problems, ASME, San Antonio (Texas), p 1–46, 1980.

[45] Cappel J., Weinberg M., Flender R., “The metallurgy of roller-bearing steels”, Steel Grips, 2, p 261–8, 2004.

[46] Ryttberg K., Knutson Wedel M., Recina V., Dahlman P., Nyborg L., “The effect of cold ring rolling on the evolution of microstructure and texture in 100Cr6 steel”, Mater. Sci. Eng., 527, p 2431–6, 2010.

[47] Stickels C.A., “Carbide refining heat treatment for 52100 bearing steels”, Metall. Trans., 5, p 865–74, 1974.

[48] Luty W., “Effect of bainitic initial structure on the properties of rolling bearing steel closer to the conventional curing”, Härterei-technische Mitteilungen, 32, p 210-4, 1977.

[49] Ipatova V.N. “Effect of a repeat annealing on the carbide network in bearing steels”, Stal., 12, p 1133–7, 1977.

[50] Tsubota K., Sato T., Kato Y, Hiraoka K., Hayashi R., “Bearing steels in the 21st century”, Bearing steels: into the 21st century, American Society for Testing of Materials, Pennsylvania (USA), p. 202–15, 1998.

[51] Polonsky I.A., Keer L.M., “On white etching band formation in rolling bearings”, J. Mech. Phys. Solids, 43, p 637, 1995.

[52] Borchers V.H., Doffin K., “Kinetik der bildung des karbids Fe_2C in stahl 100Cr6”, Archiv für das Eisenhüttenwesen, 40, p 493–8, 1969.

[53] Baracaldo R.R., Marrero J., Paramo J., “Studying the Hall-Petch effect regarding sub-micrometer steel (0.6% C)”, Bogota, vol.31, 2011.

CURRICULUM VITAE

PERSONAL INFORMATION

Name Surname : Buğra İPEK

EDUCATION

High School : Tuzluçayır Anatolian High School (2008-2012)

Bachelor : Ankara Yıldırım Beyazıt University (2012-2018)

Master Degree : Ankara Yıldırım Beyazıt University (2018-2021)

WORK EXPERIENCE

Metallurgical Laboratory Senior Engineer : Ortadoğu Rulman Sanayi ve Tic. A.Ş. (July 2021 - resuming)

Metallurgical Laboratory Engineer : Ortadoğu Rulman Sanayi ve Tic. A.Ş. (July 2018 - July 2021)

TOPIC OF INTEREST

- Steels and Alloys
- Ceramic Coatings
- Heat Treatment